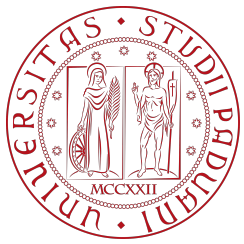

UNIVERSITÀ DEGLI STUDI DI PADOVA

Dipartimento di Fisica e Astronomia "Galileo Galilei"

Corso di Laurea in Fisica

Tesi di Laurea

Modi quasi-normali dei buchi neri

Black hole quasinormal modes

Relatore

Dr. Davide Cassani

Laureando

Michele Maserati

Anno Accademico 2023/2024

Riassunto

Questa tesi approfondisce i modi quasi-normali dei buchi neri, le oscillazioni caratteristiche di questi sistemi. Il primo passo è introdurre il formalismo necessario per trattare le perturbazioni nel contesto della relatività generale, in particolare per i buchi neri di Kerr. Per poter ottenere un'equazione differenziale separabile è necessario presentare il formalismo di Newman-Penrose, che ci permette di ricavare l'equazione di Teukolsky. Da questa possiamo ridurci a studiare due equazioni differenziali accoppiate, una per la variabile angolare (l'altro angolo e il tempo vengono trattati sfruttando le simmetrie del problema) e una per quella radiale. Gli autovalori di queste equazioni ci permettono di trovare le frequenze dei modi quasi-normali. Quest'ultime, a causa della presenza dell'orizzonte degli eventi che rende il problema non Hermitiano, hanno una parte reale e una parte immaginaria (negativa), che descrive uno smorzamento esponenziale del modo nel tempo, da cui il nome quasi-normali. Successivamente, presentiamo i metodi numerici impiegati per calcolare le frequenze dei modi quasinormali. Il metodo di Leaver riduce il problema al calcolo delle radici di una frazione continua, mentre l'approssimazione WKB fornisce un'utile stima analitica. Concentrandoci sui buchi neri di Kerr, suddividiamo l'analisi in più regimi: non estremale, quasi estremale ed estremale. Nel primo regime, implementiamo il metodo di Leaver per determinare lo spettro e lo confrontiamo con i risultati dell'approssimazione WKB. Nel regime quasi estremale, sempre studiato con il metodo di Leaver, lo spettro dei modi quasinormali presenta un comportamento peculiare: all'aumentare del parametro di rotazione, emergono due classi distinte di modi. I primi, detti damping modes, mantengono una parte immaginaria non nulla anche in prossimità dell'estremalità, mentre gli altri, gli zero-damping modes, tendono a frequenze reali. Per stabilire se le frequenze nel caso estremale siano ottenibili come limite di quelle del caso quasi estremale, introduciamo un nuovo metodo, ispirato a quello di Leaver, che sfrutta una diversa frazione continua. Questo nuovo approccio si rende necessario poiché il metodo di Leaver originario non è applicabile a questo caso. Applicando il nuovo metodo, osserviamo che i damped modes nel caso estremale rappresentano effettivamente il limite di quelli ottenuti nel regime quasi estremale. Per gli zero-damping modes non è possibile giungere a una conclusione analoga, poiché anche questo metodo fallisce. Ciononostante, sappiamo che nel limite estremale gli zero-damping modes tendono a un valore noto sull'asse reale, quindi possiamo inserire questo valore nell'equazione di Teukolsky e verificare che le soluzioni corrispondenti soddisfino le condizioni al contorno. Si dimostra che queste non sono rispettate, indicando che queste frequenze sono associate a modi di scattering piuttosto che a veri e propri modi quasinormali. I risultati numerici sono ottenuti attraverso calcoli indipendenti in cui abbiamo implementato i metodi descritti utilizzando `Mathematica` e concordano perfettamente con la letteratura.

Contents

Introduction

The study of characteristic oscillations is a powerful tool for understanding the properties of various physical systems. By analyzing the absorbed and emitted waves, we can infer important physical characteristics of the source. This thesis focuses on black holes, unique solutions to Einstein's field equations of general relativity. These objects are characterized by a spacetime singularity behind an event horizon, a boundary nothing can escape from, not even light. In our perturbation problem we must consider the horizon as a one-way membrane, making the eigenvalue problem non-Hermitian. This prevents a normal mode analysis, as the frequencies have a non-zero (negative) imaginary part. This indicates that the modes are inherently dissipative, hence the term quasinormal modes. These features make quasinormal modes an interesting subject, with a rich phenomenology that gives us insight on the underlying geometry of the spacetime. This research topic was born in the 1950s with the development of the first techniques for studying perturbations of the Schwarzschild metric by Regge and Wheeler. Since then, the field has grown and several methods were developed or imported from other fields in order to study different types of black holes and spacetime geometries. Recently, interest in quasinormal modes has grown once more, and they represent an interesting field of research. Quasinormal modes of black holes are crucial for astrophysics, particularly in gravitational wave astronomy. Black hole mergers produce signals detectable by interferometers, and quasinormal modes describe the final stage of the merger, known as the ringdown. Analyzing the frequencies and damping rates of these modes allows us to infer the mass, spin, and other properties of the resulting black hole. Modeling and characterizing quasinormal modes are essential for understanding black holes, as gravitational wave astronomy is rapidly advancing, representing a fundamental tool to study these systems, as only indirect effects can be detected in the electromagnetic spectrum. This thesis focuses on rotating neutral black holes, known as Kerr black holes, though research is active also for other types of geometries, such as the Reissner-Nordström or the Kerr-Newman metrics. Kerr black holes have an upper limit on their angular momentum determined by their mass. Black holes with the maximum possible angular momentum compatible with their mass are called extremal, and while astrophysical processes cannot accelerate these objects to exact extremality, highly spinning near-extremal black holes do exist. Extremal black holes are also valuable for studying quantum gravity effects: in the extremal limit black holes have a vanishing Hawking temperature and do not radiate, making them a perfect toy models to study the phenomenology of quantum gravity [1–3].

This work reviews and compares with concrete calculations different methods for computing the Kerr quasinormal modes, focusing on the peculiarities of the near-extremal and strictly extremal limits. In chapter 1 we introduce perturbation theory for rotating black holes, which are our main object of study. In this framework, we present the boundary conditions that define quasinormal modes, based on the physical properties of the system we are considering. Here, the event horizon plays a key role, as we must impose the absence of outgoing modes at this point, meaning our modes will decay exponentially in time. Then, we introduce the formalism necessary to obtain a manageable differential equation. In particular, we present the Newman-Penrose formalism and Petrov's classification to obtain the Teukolsky master equation, a separable partial differential equation, whose eigenvalues will give us the modes' frequencies. In chapter 2, we derive two methods which allow us to calculate the values of quasinormal frequencies: Leaver's continued fraction method and the WKB approximation, familiar from quantum mechanics. Using these two methods separately we compute the spectra of Schwarzschild and non-extremal Kerr black holes, and then compare results to test the accuracy of the WKB approximation. Our results are obtained through an independent calculation, performed with `Mathematica` notebooks, aimed at reproducing numerical results in the existing literature, particularly in [4–6]. What we find is perfect accord with the literature. In chapter 3, we use Leaver's method to calculate the near-extremal spectrum and introduce a modified continued fraction method which allows us to deal with the extremal case. In the near-extreme regime, we see emerge a class of modes whose imaginary part tends to zero as we approach extremality, resulting in a bifurcation of the spectrum. As in the chapter before, we use methods from the literature, but we do our calculations independently, finding perfect accord, for example see [7, 8]. Finally, we discuss boundary conditions for these modes in the extremal case, proving that some of these frequencies actually correspond to scattering modes.

1. Black hole perturbation theory

Our objective in this section is to solve the linearized Einstein's equations around a Kerr black hole. Following [9] we build the tools needed to study black hole perturbations, and define black hole quasinormal modes. First we introduce the Kerr metric (which is the main object of our study) as a solution to Einstein's field equations, and then we develop the formalism needed to obtain a differential equation that is sufficiently manageable. We find that the characteristic modes of the system are described by a discrete set of complex frequencies, whose imaginary parts are negative, therefore describing an exponential decay in time. These frequencies can be ordered in decreasing magnitude of the imaginary part (at least for slowly spinning black holes, we will see how this changes when we approach extremality), and numbered by an overtone number n.

1.1 Linear perturbations of the Kerr black hole

The action that describes our problem is the following (we do not consider the cosmological constant Λ):

$$S = \frac{1}{16\pi G}\int d^4x\sqrt{-g}R + \int d^4x\sqrt{-g}L[\Phi^i_M, g_{\mu\nu}], \tag{1.1}$$

where $g_{\mu\nu}$ is the metric, g its determinant, R the Ricci scalar and $L[\Phi^i_M, g_{\mu\nu}]$ the lagrangian density of matter fields Φ^i_M. The index i allows us to change the nature of the fields, which in this thesis will only be scalar, electromagnetic or gravitational. Varying the action with respect to $g_{\mu\nu}$ gives Einstein's equations (see for example [10] for a detailed derivation):

$$R_{\mu\nu} - \frac{1}{2}Rg_{\mu\nu} = 8\pi G T_{\mu\nu}, \tag{1.2}$$

while varying with respect to Φ gives the equation of motion for the matter field. We will work with Kerr black holes, whose metric can be expressed in Boyer-Lindquist coordinates (t, r, θ, ϕ) and geometrized units ($G = c = 1$) as

$$ds^2 = -\left(1 - \frac{2Mr}{\rho^2}\right)dt^2 - \frac{4Mar\sin^2\theta}{\rho^2}dtd\phi + \frac{\rho^2}{\Delta}dr^2 + \rho^2 d\phi^2 + \left(\frac{r^2 + a^2 + 2Ma^2r\sin^2(\theta)}{\rho^2}\right)\sin^2\theta d\phi^2, \tag{1.3}$$

where $a = \frac{J}{M}$ (J being the angular momentum of the black hole and M its mass), $\rho^2 = r^2 + a^2\cos^2\theta$, $\Delta = r^2 - 2Mr + a^2$. In these coordinates the event horizons occur at those fixed values of r for which $g^{rr} = 0$, that is when $\Delta(r) = 0$. This means we have two horizons, an inner and an outer one, respectively at r_- and r_+, given by $r_\pm = M \pm \sqrt{M^2 - a^2}$. In general $a/M \leq 1$, if $a/M = 1$, the system is said to be extremal and at this limit $r_- = r_+$. This is the maximum possible value of a/M for any physical black hole, as at higher values we would have a naked singularity, a singularity without an event horizon [10].

In order to study perturbations of this system, we introduce the following notation: "background" refers to all unperturbed quantities $\bar{g}_{\mu\nu}$, $\bar{\Phi}^i_M$, and since we want to study the intrinsic oscillations of the black hole, we will put $\bar{\Phi}^i_M = 0$. We can then write perturbations of these quantities as follows:

$$g_{\mu\nu} = \bar{g}_{\mu\nu} + h_{\mu\nu}, \qquad \Phi^i_M = \bar{\Phi}^i_M + \delta\Phi^i_M,$$

where $h_{\mu\nu}$ and $\delta\Phi^i_M$ are small.

The metric has two Killing vectors ∂_t and ∂_θ, meaning there is not an explicit dependence on t or ϕ in the equations and we can perform a Fourier transform. Since ϕ is a periodic coordinate with period 2π, we have a discrete sum over the Fourier modes (indexed by m). We can collectively denote the metric and the matter fields as $\Phi^i(t, r, \theta, \phi)$ and obtain:

$$\Phi^i(t, r, \theta, \phi) = \frac{1}{2\pi}\int d\omega e^{-i\omega t}\sum_{m\in\mathbb{Z}} e^{im\phi}F^i(r, \theta). \tag{1.4}$$

Before writing the physical boundary conditions, let us introduce a set of convenient coordinates $(v_*, r_*, \theta, \phi_*)$, called the Eddington-Finkelstein coordinates. r_* is called tortoise coordinate, $v_* = t + r_*$, and the following hold:

$$dr_* := \frac{r^2 + a^2}{\Delta} dr, \qquad d\phi_* := d\phi + \frac{a}{\Delta} dr. \tag{1.5}$$

The first condition we must impose is

$$e^{-i\omega t + im\phi} F(r, \theta) \xrightarrow{r \to r_+} e^{-i\omega v_* + im\phi} F(\theta). \tag{1.6}$$

This means that there are only modes which go into the black hole at the event horizon. We also want to prevent the stimulated emission of the black hole, meaning we only want to study intrinsic emissions of the system. Thus, we ask to only have outgoing modes at infinity (problems where the black hole reacts to waves coming from spatial infinity are scattering problems, which we will not discuss):

$$e^{-i\omega t + im\phi} F(r, \theta) \xrightarrow{r \to \infty,\ u \text{ fixed}} e^{-i\omega u + im\phi} \tilde{F}(\theta), \tag{1.7}$$

where $u = t - r$ is called asymptotically flat retarded time. Now, we would be tempted to linearize Einstein's equations keeping terms up to first order in $h_{\mu\nu}$ and $\delta\Phi^i_M$, however we would get a quite complicated system of coupled differential equations. In 1973, Teukolsky found a way to overcome this problem and obtain decoupled differential equation using a different formalism, called Newman-Penrose (NP) formalism, which is the object of the next section [11].

1.1.1 Newman-Penrose formalism and Petrov's classification

In order to obtain the Teukolsky master equation, we need to give an introduction to a useful formalism in general relativity, the tetrad formalism. We will be very brief, for a more extensive introduction see for example [10] for the tetrad formalism and [9, 12] for the Newman-Penrose formalism (introduced later in this section).

In this framework, our quantities are not expressed as functions of the metric $g_{\mu\nu}$, but we work in a coordinate free system: the elements of the basis of such system are called tetrads. The formal definition goes as follows. Given a manifold and its tangent space T_p at point p, we define a tetrad as a basis for the tangent space $\hat{e}_{(a)}$, $a = 0, 1, 2, 3$ which satisfies

$$g(\hat{e}_{(a)}, \hat{e}_{(b)}) = \eta_{ab}, \tag{1.8}$$

where η_{ab} is the Minkowski metric of the tangent space at each point and $g(\ ,\ )$ is the usual metric tensor. We can express the our basis vectors $\hat{e}_{(\mu)} = \partial_\mu$ in terms of the tetrads:

$$\hat{e}_{(\mu)} = e_\mu{}^a \hat{e}_{(a)}, \tag{1.9}$$

$e_\mu{}^a$ is an invertible matrix and with a small abuse of notation we will refer to $e_\mu{}^a$ as the tetrad. We will denote its inverse as $e^\mu{}_a$, which satisfies:

$$e^\mu{}_a e_\nu{}^a = \delta^\mu_\nu \qquad e_\mu{}^a e^\mu{}_b = \delta^a_b. \tag{1.10}$$

We can also rewrite (1.8) as

$$g_{\mu\nu} e^\mu{}_a e^\nu{}_b = \eta_{ab}, \qquad \text{or equivalently} \qquad g_{\mu\nu} = e_\mu{}^a e_\nu{}^b \eta_{ab}. \tag{1.11}$$

The Newman-Penrose (NP) formalism is a tetrad formalism with complex tetrads and Minkowski metric at every point

$$\eta_{ab} = \begin{pmatrix} 0 & -1 & 0 & 0 \\ -1 & 0 & 0 & 0 \\ 0 & 0 & 0 & 1 \\ 0 & 0 & 1 & 0 \end{pmatrix}. \tag{1.12}$$

The tetrad is a set of 4 null vectors $l_\mu, n_\mu, m_\mu, \bar{m}_\mu$ with

$$g_{\mu\nu} = -l_\mu n_\nu - n_\mu l_\nu + m_\mu \bar{m}_\nu + \bar{m}_\mu m_\nu, \tag{1.13}$$

where l_μ and n_μ are real, m_μ and $\bar{m}_\mu$ are complex conjugated [12]. Now, we need to redefine parallel transport in terms of this formalism, so we define 4 locally defined directional derivatives:

$$D = l^\mu \nabla_\mu \quad \Delta = n^\mu \nabla_\mu \quad \delta = m^\mu \nabla_\mu \quad \bar{\delta} = \bar{m}^\mu \nabla_\mu. \tag{1.14}$$

In this formalism, instead of using Christoffel symbols (which have 24 components) we define 12 complex spin coefficients which are:

$$\kappa = -m^\mu l^\nu \nabla_\nu l_\mu, \quad \sigma = -m^\mu m^\nu \nabla_\nu l_\mu, \quad \epsilon = -\frac{1}{2}(n^\mu l^\nu \nabla_\nu l_\mu + m^\mu l^\nu \nabla_\nu \bar{m}_\mu), \tag{1.15}$$

$$\lambda = -n^\mu \bar{m}^\nu \nabla_\nu \bar{m}_\mu, \quad \nu = -n^\mu n^\nu \nabla_\nu \bar{m}_\mu, \quad \gamma = -\frac{1}{2}(n^\mu n^\nu \nabla_\nu l_\mu + m^\mu n^\nu \nabla_\nu \bar{m}_\mu, \tag{1.16}$$

$$\rho = -m^\mu \bar{m}^\nu \nabla_\nu l_\mu, \quad \mu = -n^\mu m^\nu \nabla_\nu \bar{m}_\mu, \quad \alpha = -\frac{1}{2}(n^\mu \bar{m}^\nu \nabla_\nu l_\mu + m^\mu \bar{m}^\nu \nabla_\nu \bar{m}_\mu), \tag{1.17}$$

$$\tau = -m^\mu n^\nu \nabla_\nu l_\mu, \quad \pi = -n^\mu l^\nu \nabla_\nu \bar{m}_\mu, \quad \beta = -\frac{1}{2}(n^\mu m^\nu \nabla_\nu l_\mu + m^\mu m^\nu \nabla_\nu \bar{m}_\mu). \tag{1.18}$$

We also wan to to introduce a new object, in place of the Riemann tensor, called Weyl tensor, which represents the traceless part of the Riemann tensor. It is defined as

$$W_{\mu\nu\rho\sigma} = R_{\mu\nu\rho\sigma} - g_{\mu[\rho} R_{\sigma]\nu} + g_{\nu[\rho} R_{\sigma]\mu} + \frac{1}{3} R g_{\mu[\rho} g_{\sigma]\nu}. \tag{1.19}$$

The Weyl tensor has 10 independent components, which can be described through 5 complex scalars defined in the NP formalism as follows:

$$\begin{aligned} \psi_0 = W_{\alpha\beta\gamma\delta} l^\alpha m^\beta l^\gamma m^\delta, \qquad \psi_1 = W_{\alpha\beta\gamma\delta} l^\alpha n^\beta l^\gamma m^\delta, \qquad \psi_2 = W_{\alpha\beta\gamma\delta} l^\alpha m^\beta \bar{m}^\gamma n^\delta, \\ \psi_3 = W_{\alpha\beta\gamma\delta} l^\alpha n^\beta \bar{m}^\gamma n^\delta, \qquad \psi_4 = W_{\alpha\beta\gamma\delta} n^\alpha \bar{m}^\beta n^\gamma \bar{m}^\delta. \end{aligned} \tag{1.20}$$

This object, as it is not dependent on matter fields, represents the purely gravitational field. For example, for every void solution ($T_{\mu\nu} = 0$) the Ricci tensor is always zero, while the Weyl tensor may be non-vanishing. One last part of formalism we need is the Petrov's classification, which is an algebraic, coordinate-independent, classification of solutions to Einstein's equations, which Petrov obtained using NP formalism in 1954 [13]. We mention here only the results which are useful in our derivation of Teukolsky equation, a more in depth introduction can be found in [9].

There are three equivalent formulations of such classification. The first one, due to Petrov, classifies the Weyl tensor by the number of degenerate local eigenvalues and (antisymmetric) eigenbivectors of the Weyl tensor. The eigenvalue equation is $W^{\mu\nu}{}_{\alpha\beta} X^{\alpha\beta} = \lambda X^{\mu\nu}$. Another formulation follows from a result by Penrose (1960) which proves that this problem is equivalent to the classification of spacetimes based on the number of principal null directions of the Weyl tensor. The null vectors that span these directions are given by $k_{[\alpha} W_{\beta]\gamma\delta[\rho} k_{\sigma]} k^\gamma k^\delta = 0$. The last formulation, and the one that is most useful to us, relates the classification of the spacetime solutions to the five Weyl-Newman-Penrose scalars 1.20, namely to how many of these scalars can be made zero for a given spacetime by a suitable orientation of the tetrad frame. In particular, the Kerr spacetime is called a Petrov type D spacetime, meaning it has two distinct but double degenerate principal null directions, and thus we can find a tetrad where ψ_2 is the only non-vanishing scalar [9].

1.2 Teukolsky equation

We now present a derivation of Teukolsky equation for gravitational perturbations following [11]. The derivation of the equation for the other types of fields can be found in [11] for the electromagnetic case and [9] for the scalar case, other types of fields are discussed in [11, 14]. The gravitational quantities we will focus on are

$$\psi_0 = -W_{\mu\nu\rho\sigma} l^\mu m^\nu l^\rho m^\sigma, \qquad \psi_4 = -W_{\mu\nu\rho\sigma} n^\mu \bar{m}^\nu n^\rho \bar{m}^\delta, \tag{1.21}$$

In fact, these are the only two scalars whose perturbations can be studied by performing a simple analysis without any additional information on how the mass and the angular momentum of the

black hole M and J change. Instead of acting on the metric writing $g_{\mu\nu} = \bar{g}_{\mu\nu} + h_{\mu\nu}$, we perturb the tetrad components $l = l^A + l^B$ and so on, with the quantities denoted with the apex ^{B} small, and we keep everything up to first order. Our perturbation equations are therefore of the form $\psi_0 = \psi_0^A + \psi_0^B$, $D = D^A + D^B$, ...

Since the Kerr black hole is a Type D spacetime, we know we can choose two principal null directions of the Weyl tensor so that only $\psi_2^A \neq 0$, in particular these will be l_μ and n_μ and therefore:

$$\psi_0^A = \psi_1^A = \psi_3^A = \psi_4^A = 0, \qquad \kappa^A = \sigma^A = \nu^A = \lambda^A = 0. \tag{1.22}$$

We have the following three non vacuum equations, which can be obtained by rewriting Bianchi's identity and the Einstein's equations in terms of NP quantities (see [11, 14] for the derivation):

$$\begin{aligned}(\bar{\delta} - 4\alpha + \pi)\psi_0 - (D - 4\rho - 2\epsilon)\psi_1 - 3\kappa\psi_2 = (\delta + \bar{\pi} - 2\bar{\alpha} - 2\beta)\Phi_{00} - (D - 2\epsilon - 2\bar{\rho})\Phi_{01} + \\ + 2\sigma\Phi_{10} - 2\kappa\Phi_{11} - \bar{\kappa}\Phi_{02},\end{aligned} \tag{1.23}$$

$$\begin{aligned}(\Delta - 4\gamma + \mu)\psi_0 - (\delta - 4\tau - 2\beta)\psi_1 - 3\sigma\psi_2 = (\delta + 2\bar{\pi} - 2\beta)\Phi_{01} - (D - 2\epsilon + 2\bar{\epsilon} - \bar{\rho})\Phi_{02} + \\ - \bar{\lambda}\Phi_{00} + 2\sigma\Phi_{11} - 2\kappa\Phi_{12},\end{aligned} \tag{1.24}$$

$$(D - \rho - \bar{\rho} - 3\epsilon + \bar{\epsilon})\sigma - (\delta - \tau + \bar{\pi} - \bar{\alpha} - 3\beta)\kappa - \psi_0 = 0. \tag{1.25}$$

The $\Phi_{\mu\nu}$ are given by:

$$\Phi_{\mu\nu} = -\frac{1}{2}R_{\alpha\beta}\mathcal{M}^\alpha\mathcal{V}^\beta = 4\pi T_{\alpha\beta}\mathcal{M}^\alpha\mathcal{V}^\beta = 4\pi T_{\mathcal{M}\mathcal{V}}, \tag{1.26}$$

with $\mu = 0, 1, 2, 3$, and $\mathcal{M}, \mathcal{V} = l, n, m, \bar{m}$, so for example we will have $\Phi_{00} = -1/2R_{\alpha\beta}l^\alpha l^\beta = 4\pi T_{ll}$ or $\Phi_{01} = -1/2R_{\alpha\beta}l^\alpha n^\beta$ and so on. Using this and (1.22) we can perturb (1.25) and obtain

$$(\bar{\delta} - 4\alpha + \pi)^A\psi_0^B - (D - 4\rho - 2\epsilon)^A\psi_1^B - 3\kappa^B\psi_2^A = 4\pi[(\delta + \bar{\pi} - 2\bar{\alpha} - 2\beta)^A T_{ll}^B - (D - 2\epsilon - 2\bar{\rho})^A T_{lm}^B], \tag{1.27}$$

$$(\Delta - 4\gamma + \mu)^A\psi_0^B - (\delta - 4\tau - 2\beta)^A\psi_1^B - 3\sigma^B\psi_2^A = 4\pi[(\delta + 2\bar{\pi} - 2\beta)^A T_{lm}^B - (D - 2\epsilon + 2\bar{\epsilon} - \bar{\rho})^A T_{mm}^B], \tag{1.28}$$

$$(D - \rho - \bar{\rho} - 3\epsilon + \bar{\epsilon})^A\sigma^B - (\delta - \tau + \bar{\pi} - \bar{\alpha} - 3\beta)^A\kappa^B - \psi_0^B = 0. \tag{1.29}$$

To simplify notation, we will now drop the label A from background quantities. The background ψ_2 satisfies

$$D\psi_2 = 3\rho\psi_2, \qquad \delta\psi_2 = 3\tau\psi_2. \tag{1.30}$$

Therefore, we have that (1.29) can be written as

$$(D - 3\epsilon + \bar{\epsilon} - 4\rho - \bar{\rho})\psi_2\sigma^B - (\delta + \bar{\pi} - \bar{\alpha} - 3\beta - 4\tau)\psi_2\kappa^B - \psi_0^B\psi_2 = 0. \tag{1.31}$$

Now we want to eliminate ψ_1^B from (1.27) and (1.28). This can be done using the commutation relation obtained by Teukolsky in [11]:

$$[D - (p+1)\epsilon + \bar{\epsilon} + q\rho - \bar{\rho}](\delta - p\beta + q\tau) - [\delta - (p+1)\beta - \bar{\alpha} + \bar{\pi} + q\tau](D - p\epsilon + q\rho) = 0, \tag{1.32}$$

where p, q are two constants. Therefore, we can apply $(D - 3\epsilon + \bar{\epsilon} - 4\rho - \bar{\rho})$ on (1.28) and $(\delta + \bar{\pi} - \bar{\alpha} - 3\beta - 4\tau)$ on (1.27) and subtract one from the other. What we get is:

$$\begin{aligned}&[(D - 3\epsilon + \bar{\epsilon} - 4\rho - \bar{\rho})(\Delta - 4\gamma + \mu) - (\delta + \bar{\pi} - \bar{\alpha} - 3\beta - 4\tau)(\bar{\delta} + \pi - 4\alpha) - 3\psi_2]\psi_0^B \\ &+ \{[D - 3\epsilon + \bar{\epsilon} - 4\rho - \bar{\rho}](\delta - 2\beta - 4\tau) - [\delta - 3\beta - \bar{\alpha} + \bar{\pi} - 4\tau](D - 2\epsilon - 4\rho)\}\psi_1^B \\ &+ [(D - 3\epsilon + \bar{\epsilon} - 4\rho - \bar{\rho})\psi_2\sigma^B - (\delta + \bar{\pi} - \bar{\alpha} - 3\beta - 4\tau)\psi_2\kappa^B - \psi_0^B\psi_2] = 4\pi T_0,\end{aligned} \tag{1.33}$$

where the coefficient of ψ_1^B is 0 because of (1.32) (with p=2, q=-4), and terms with ψ_2 cancel out because of (1.31). We have also defined

$$\begin{aligned}T_0 = (\delta + \bar{\pi} - \bar{\alpha} - 3\beta - 4\tau)[(D - 2\epsilon - 2\bar{\rho})T_{lm}^B - (\delta + \bar{\pi} - 2\bar{\alpha} - 2\beta)T_{ll}^B] \\ + (D - 3\epsilon + \bar{\epsilon} - 4\rho - \bar{\rho})[(\delta + 2\bar{\pi} - 2\beta)T_{lm}^B - (D - 2\epsilon + 2\bar{\epsilon} - \bar{\rho})T_{mm}^B].\end{aligned} \tag{1.34}$$

We are then left with

$$[(D-3\epsilon+\bar{\epsilon}-4\rho-\bar{\rho})(\Delta-4\gamma+\mu)-(\delta+\bar{\pi}-\bar{\alpha}-3\beta-4\tau)(\bar{\delta}+\pi-4\alpha)-3\psi_2]\psi_0^B=4\pi T_0. \quad (1.35)$$

This is the decoupled equation for ψ_0^B. From this, we can derive an analogous result for ψ_4^B by applying this transformation: $l \longleftrightarrow n, \quad m \longleftrightarrow \bar{m}$. All NP equations are invariant under this transformation and this symmetry is not broken by choosing the null directions which determine Eq. (1.22) [15]. We get:

$$[(\Delta+3\gamma-\bar{\gamma}+4\mu+\bar{\mu})(D+4\epsilon-\rho)-(\bar{\delta}-\bar{\tau}+\bar{\beta}+3\alpha+4\pi)(\delta-\tau+4\beta)-3\psi_2]\psi_4^B=4\pi T_4, \quad (1.36)$$

where

$$\begin{aligned} T_4 = {} & (\Delta+3\gamma-\bar{\gamma}+4\mu+\bar{\mu})[(\bar{\delta}-2\bar{\tau}+2\alpha)T_{n\bar{m}}-(\Delta+2\gamma-2\bar{\gamma}+\bar{\mu})T_{\bar{m}\bar{m}}] \\ & +(\bar{\delta}-\bar{\tau}+\bar{\beta}+3\alpha+4\pi)[(\Delta+2\gamma+2\bar{\mu})T_{n\bar{m}}-(\bar{\delta}-\bar{\tau}+2\bar{\beta}+2\alpha)T_{nm}]. \end{aligned} \quad (1.37)$$

Now, we want to write our result in a Boyer-Lindquist coordinates (t, r, θ, ϕ). One possible choice of the tetrad components is the so called Kinnersley tetrad (see appendix A of [11] for a detailed discussion of the degrees of freedom), where we have:

$$l^\mu=(\frac{r^2+a^2}{\Delta},1,0,\frac{a}{\Delta}), \quad n^\mu=\frac{(r^2+a^2,-\Delta,0,a)}{2\Sigma}, \quad m^\mu=\frac{(ia\sin\theta,0,1,i/\sin\theta)}{\sqrt{2}(r+ia\cos\theta)}. \quad (1.38)$$

The only nonzero Weyl component is $\psi_2=M\rho^3$, and the non-zero spin coefficients are

$$\begin{gathered} \rho=-\frac{1}{r-ia\cos\theta}, \quad \beta=-\frac{\bar{\rho}\cot\theta}{2\sqrt{2}}, \quad \pi=\frac{ia\rho^2\sin\theta}{\sqrt{2}}, \quad \tau=-\frac{ia\rho\bar{\rho}\sin\theta}{\sqrt{2}}, \\ \mu=\frac{\rho^2\bar{\rho}\Delta}{2}, \quad \gamma=\mu+\frac{\rho\bar{\rho}(r-M)}{2}, \quad \alpha=\pi-\bar{\beta}. \end{gathered} \quad (1.39)$$

We can use these expressions, together with the definition of D, Δ, δ to obtain the Teukolsky master equation. It is pretty convenient to write the equation in the following form, allowing for a more general discussion of massless perturbation for different spins:

$$\begin{aligned} & \left[\frac{(r^2+a^2)^2}{\Delta}-a^2\sin^2\theta\right]\frac{\partial^2\psi}{\partial t^2}+\frac{4Mar}{\Delta}\frac{\partial^2\psi}{\partial t\partial\phi}+\left[\frac{a^2}{\Delta}-\frac{1}{\sin^2\theta}\right]\frac{\partial^2\psi}{\partial\phi^2} \\ & -\Delta^{-s}\frac{\partial}{\partial r}\left(\Delta^{s+1}\frac{\partial\psi}{\partial r}\right)-\frac{1}{\sin\theta}\frac{\partial}{\partial\theta}\left(\sin\theta\frac{\partial\psi}{\partial\theta}\right)-2s\left[\frac{a(r-M)}{\Delta}+\frac{i\cos\theta}{\sin^2\theta}\right]\frac{\partial\psi}{\partial\phi} \\ & -2s\left[\frac{M(r^2-a^2)}{\Delta}-r-ia\cos\theta\right]\frac{\partial\psi}{\partial t}+(s^2\cot^2\theta-s)\psi=T. \end{aligned} \quad (1.40)$$

Based on the value of s, by choosing the appropriate form ψ and T one can describe gravitational ($s=\pm2$, we derived both these equations, one is the equation for ψ_0, the other for ψ_4), electromagnetic $s=\pm1$ or scalar ($s=0$) perturbations. The equation also has physical meaning for fractional values $s=1/2,\ 3/2$ But these will not be considered in this thesis. Some values for ψ are in Table 1.1, while since we will set $T=0$ we will not worry about it. All these values for ψ and the ones for T can be found in [4, 14, 16].

Table 1.1: Teukolsky wavefunction ψ for each value s of the spin. The spin-coefficient $\rho\equiv-1/(r-ia\cos\theta)$. The quantities Φ_0 and Φ_1 are defined from the Maxwell tensor as $\Phi_0=F_{\mu,\nu}l^\mu m^\nu$, $\Phi_2=F_{\mu\nu}\bar{m}^\mu n^\nu$

s	0	$(+1,-1)$	$(+2,-2)$
ψ	Φ	$(\Phi_0,\rho^{-2}\Phi_2)$	$(\psi_0,\rho^{-4}\psi_4)$

An important note is that there are relations between the solutions with $+s$ and $-s$, the Teukolsky-Starobinsky identities, which allow us to only study either positive or negative values of s without losing any physical information [17].

Using Fourier transform we can write the general solution to the Teukolsky equation in the separable form

$$\psi(t,r,\theta,\phi) = \frac{1}{2\pi}\int d\omega e^{-i\omega t}\sum_{l=|s|}^{\infty}\sum_{m=-l}^{+l} e^{im\phi}R^s_{lmw}(r)S^s_{lmw}(\cos\theta). \tag{1.41}$$

Plugging this in the equation we obtain the so called angular and radial equations, which are

$$\left[\frac{d}{dx}(1-x^2)\frac{d}{dx}\right]S^s_{lm\omega} + \left[a^2\omega^2x^2 - 2a\omega sx + s + A^s_{lm} - \frac{(m+sx)^2}{1-x^2}\right]S^s_{lm\omega} = 0, \tag{1.42}$$

$$\Delta^{-s}\frac{\partial}{\partial r}\left(\Delta^{s+1}\frac{\partial R^s_{lm\omega}}{\partial r}\right) - V(r)R^s_{lm\omega}(r) = T_{lm\omega}(r), \tag{1.43}$$

where $x = \cos\theta$, source $T_{lmw}(r)$ and potential

$$V(r) = -\frac{(K_{m\omega})^2 - 2si(r-M)K_{m\omega}}{\Delta} - 4siwr + \lambda_{lm\omega}, \tag{1.44}$$

$$K_{mw} = (r^2+a^2)\omega - ma, \quad \lambda_{lm\omega} = A^s_{lm\omega} - 2am\omega + a^2\omega^2. \tag{1.45}$$

We have been a little sloppy with indices: we should have written ω^s_{lm}, however we dropped the indices for conciseness. The angular equation is known in literature, and its solutions are called spin-weighted spheroidal harmonics (a detailed discussion of eigenvalues of such functions can be found in [18]). We state some important symmetries of this equation in terms of the angular separation constant A^s_{lm}:

- $A^s_{lm} = \bar{A}^s_{l-m}$ which relates positive and negative values of m
- $A^{-s}_{lm} = A^s_{lm} + 2s$ which relates positive and negative values of the spin weight s
- To any solution $(\omega^s_{lm}, A^s_{lm})$ corresponds another solution $(-\bar{\omega}^s_{l-m}, \bar{A}^s_{l-m})$

From now on, in order to make the notation lighter, we will write $A^s_{lm} \to A_{lm}$, $\omega^s_{lm} \to \omega$.

2. Computing QNMs: non-extremal Kerr

2.1 Leaver's continued fraction method

2.1.1 Solving the angular equation

The Teukolsky master equation offers us the starting point for our determination of quasinormal frequencies, however, we still need practical ways of computing these numbers. The main method we will use in this thesis was developed by Leaver in [19] and it allows us to calculate quasinormal modes as roots of a continued fraction. Following Leaver, to make the calculation lighter, in this section we set $M = 1/2$ (however we will always plot $M\omega$, so that it is easy to generalize the results for different values of M). As we said before, the solutions of (1.42) $S^s_{lm\omega}(x)$ ($x = \cos\theta$) are called spin-weighted spheroidal harmonic, which, for any fixed value of s, form an orthogonal set of functions in the interval $[-1, 1]$, that is:

$$\int_{-1}^{1} dx S^s_{lm\omega}(x) S^s_{l'm'\omega'}(x) = \delta_{ll'}\delta_{mm'}\delta(\omega - \omega'). \tag{2.1}$$

The parameters l, m only take integer values, and it must hold $l \geq s$ and $|m| \leq l$ (otherwise the function is identically null) [18]. When $s = 0$ the functions are the so-called spheroidal harmonics. We are interested in finding semi-analytical approximations to our solution, and one solution can be found using the Frobenius method. This method allows us to solve second order differential equation in the form

$$V(x)y'' + P(x)y' + Q(x)y = 0. \tag{2.2}$$

The theorem of Frobenius states that if, for $x_0 : V(x_0) = 0$, $\lim_{x\to x_0}(x-x_0)P(x)/V(x)$ and $\lim_{x\to x_0}(x-x_0)^2Q(x)/V(x)$ exist (meaning x_0 is a regular singular point), we can write a solution to the equation as a power series around x_0 (see [20] for a more formal statement of the theorem). Our equation (1.42) has two regular singular points at $x = \pm 1$, and an irregular one at $x = \infty$, and we impose boundary conditions such that the solution is well behaved at these points (we want it to be finite). Lets start with $x = +1$. If we consider only the dominant terms in the equation as $x \to 1$ we have

$$\left[\frac{d}{dx}(1-x^2)\frac{d}{dx}\right] S^s_{lm\omega}(x) - \frac{m^2 + 2msx + s^2}{1-x^2} S^s_{lm\omega}(x) = 0. \tag{2.3}$$

Always for $x \to 1$ we can write

$$4(1-x)^2\frac{d^2}{dx^2}S^s_{lm\omega}(x) - 4(1-x)\frac{d}{dx}S^s_{lm\omega}(x) - (m+s)^2 S^s_{lm\omega}(x) = 0, \tag{2.4}$$

which implies an asymptotic behaviour of $S^s_{lm\omega}(x) \sim (1+x)^{\pm\frac{1}{2}|m+s|}$ as $x \to 1$. Similarly, we can obtain that for $x \to -1$ we have $S^s_{lm\omega}(x) \sim (1-x)^{\pm\frac{1}{2}|m-s|}$. As x tends to ∞ the equation is again integrable and we find $S^s_{lm\omega}(x) \sim e^{ia\omega x}$. Therefore, we have a natural ansatz for the complete solution in the form:

$$S^s_{lm\omega}(x) = e^{ia\omega x}(1+x)^{\frac{1}{2}|m+s|}(1-x)^{\frac{1}{2}|m-s|}\sum_{n=0}^{+\infty} a_n(1+x)^n. \tag{2.5}$$

Then, we substitute this ansatz in our equation (1.42) and equate all terms which multiply the same power of x. It is possible to show that the coefficients of the expansion are related by the following recursion relation:

$$\begin{cases} \alpha^\theta_0 a_1 + \beta^\theta_0 a_0 = 0, \\ \alpha^\theta_n a_{n+1} + \beta^\theta_n a_n + \gamma^\theta_n a_{n-1} = 0 \quad n = 1, 2, ... \end{cases} \tag{2.6}$$

The motivation behind the apex θ, denoting we are working with the angular equation, will become evident in the next section. The explicit form of the coefficients is the following

$$\begin{cases} \alpha_n^\theta = & -2(n+1)(n+2k_1+1), \\ \beta_n^\theta = & n(n-1)+2n(k_1+k_2+1-2a\omega)-[2a\omega(2k_1+s+1)-(k_1+k_2)(k_1+k_2+1)]+ \\ & -[a^2\omega^2+s(s+1)+A_{lm}], \\ \gamma_n^\theta = & 2a\omega(n+k_1+k_2-s), \end{cases} \tag{2.7}$$

where $k_1 = \frac{1}{2}|m-s|$ and $k_2 = \frac{1}{2}|m+s|$. Now, we define $r_n = a_{n+1}/a_n$ and the second equation in (2.6) becomes $\alpha_n^\theta r_n + \beta_n^\theta + \gamma_n^\theta / r_{n-1} = 0$. Solving this for r_{n-1} gives:

$$r_{n-1} = -\frac{\gamma_n^\theta}{\beta_n^\theta + \alpha_n^\theta r_n} = -\cfrac{\gamma_n^\theta}{\beta_n^\theta - \alpha_n^\theta \cfrac{\gamma_{n+1}^\theta}{\beta_{n+1}^\theta - \alpha_{n+1}^\theta \cfrac{\gamma_{n+2}^\theta}{\cdots}}}. \tag{2.8}$$

Using the first of Eq. 2.6 we can write (using another notation for the continued fraction)

$$\frac{\beta_0}{\alpha_0} = -\frac{a_1}{a_0} = -r_0 = \cfrac{\gamma_1^\theta}{\beta_1^\theta -} \cfrac{\alpha_1^\theta \gamma_2^\theta}{\beta_2^\theta -} \cfrac{\alpha_2^\theta \gamma_3^\theta}{\beta_3^\theta -} \cdots, \tag{2.9}$$

and from this one we can solve for the angular separation constant A_{lm}. Note that the terms depend on ω, which we still do not know: as we will see in the next section, this means we have to solve the angular and radial equation simultaneously. This is not true for the Schwarzschild metric, where $a = 0$ and the radial and angular equations decouple.

2.1.2 Solving the radial equation

The radial equation can be solved in the same fashion as the angular one. In this case, the singular points are the two roots of Δ, which are the outer and inner horizons of the black hole, respectively r_+ and r_- (the event horizon and the Cauchy horizon). At $r = r_+$ the equation can be integrated giving $R^s_{lm\omega}(r) \sim r^{i\sigma_+}$ and $R^s_{lm\omega}(r) \sim r^{-s-i\sigma_+}$, where we defined $\sigma_+ = (\omega r_+ - am)/\sqrt{1-4a^2}$. The first solution must be excluded because only modes going into the horizon are allowed. We can do the same at ∞ and again we obtain two possible solutions: $R^s_{lm\omega} \sim r^{-1-2s+i\omega} e^{i\omega r}$ and $R^s_{lm\omega} \sim r^{-1-i\omega} e^{-i\omega r}$, however, the second one is discarded because the mode at infinity must be outgoing. Therefore, our ansatz can be written as:

$$R^s_{lm\omega}(r) = e^{i\omega r}(r-r_-)^{-1-s+i\omega+i\sigma_+}(r-r_+)^{-s-i\sigma_+} \sum_{n=0}^{+\infty} d_n \left(\frac{r-r_+}{r-r_-}\right)^n. \tag{2.10}$$

Note that for extremal black holes ($a/M = 1$), where $r_+ = r_-$, this method cannot work. Plugging this into the radial equation gives another recursion, similar to the first:

$$\begin{cases} \alpha_0^r d_1 + \beta_0^r d_0 = 0, \\ \alpha_n^r d_{n+1} + \beta_n^r d_n + \gamma_n^r d_{n-1} = 0, \qquad n = 1, 2, ..., \end{cases} \tag{2.11}$$

which gives rise to the following continued fraction

$$0 = \beta_0^r - \cfrac{\alpha_0^r \gamma_1^r}{\beta_1^r -} \cfrac{\alpha_1^r \gamma_2^r}{\beta_2^r -} \cfrac{\alpha_2^r \gamma_3^r}{\beta_3^r -} \cdots \tag{2.12}$$

The recurrence coefficients are ($b = \sqrt{1-4a^2}$):

$$\begin{cases} \alpha_n^r = n^2 + (c_0+1)n + c_0, \\ \beta_n^r = -2n^2 + (c_1+2)n + c_3, \\ \gamma_n^r = n^2 + (c_2-3)n + c_4 - c_2 + 2, \end{cases} \qquad \begin{cases} c_0 = & 1 - s - i\omega - \frac{2i}{b}\left(\frac{\omega}{2} - am\right), \\ c_1 = & -4 + 2i\omega(2+b) + \frac{4i}{b}\left(\frac{\omega}{2} - am\right), \\ c_2 = & s + 3 - 3i\omega - \frac{2i}{b}\left(\frac{\omega}{2} - am\right), \\ c_3 = & \omega^2(4+2b-a^2) - 2am\omega - s - 1 + (2+b)i\omega + \\ & -A_{lm} + \frac{4\omega+2i}{b}\left(\frac{\omega}{2} - am\right), \\ c_4 = & s + 1 - 2\omega^2 - (2s+3)i\omega - \frac{4\omega+2i}{b}\left(\frac{\omega}{2} - am\right). \end{cases} \tag{2.13}$$

Now we can search numerically for roots of both Eq. 2.12 and 2.9, and find the values for ω and A_{lm}.

2.2 WKB method

The WKB method is a powerful approximation which allows us to calculate quasinmormal modes in a rather simple and computationally efficient way. The first thing we need to do is to rewrite our master equation in the form

$$\frac{d^2}{dx^2}\Psi + Q(x)\Psi = 0, \tag{2.14}$$

where $Q(x)$ will be a potential function in some coordinate system, and then apply the WKB technique, first developed in quantum mechanics to solve Schrödinger's equation. This has also an intuitive interpretation: in this view, quasinormal modes are seen as stationary waves at the circular null geodesic (the light ring of the black hole) slowly leaking away [6]. This method was first introduced in the field of quasinormal modes to solve the radial equation in the case of Schwarzschild black holes [21,22]. Here, we present some results of this method which we will apply to the Kerr black hole, for a more in depth discussion of the WKB approximation and all its possible application see [23,24]. In the quantum mechanics version of the problem $Q(x) = -\frac{2m}{\hbar}[V(x) - E]$ (with E the energy of the particle, m its mass and $V(x)$ the potential) [23]. If the potential is constant the solution is a plane wave or a decaying exponential of the form $\Psi = e^{\pm i\sqrt{Q}x}$, so, if the potential is slowly varying (we will see in detail what we need as an assumption), we can guess a solution inspired by the plane waves as:

$$\Psi(x) = e^{\pm i\int_{x_0}^{x}\sqrt{Q(\xi)}d\xi}. \tag{2.15}$$

Plugging this into our differential equation we get:

$$\frac{d^2\Psi}{dx^2} + Q(x)\Psi = \left(\frac{d^2}{dx^2} + Q(x)\right)e^{\pm i\int_{x_0}^{x}\sqrt{Q(\xi)}d\xi} = \pm i\frac{Q'(x)}{2\sqrt{Q(x)}}e^{\pm i\int_{x_0}^{x}\sqrt{Q(\xi)}d\xi}, \tag{2.16}$$

meaning our approximation holds if

$$|Q'(x)/(2\sqrt{Q(x)})| \ll |Q(x)|, \tag{2.17}$$

which will be our condition to find a WKB approximation. Then, we can compute higher order approximation assuming a function as in $\Psi(x) = e^{iS(x)}$ and substitute it in the differential equation:

$$iS''(x) - S'(x)^2 + Q(x) = 0. \tag{2.18}$$

We can solve this equation using an iterative process of successive approximations:

$$S_0 = \pm\int_{x_0}^{x}\sqrt{Q(\xi)}d\xi, \quad S_n = \pm\int_{x_0}^{x}\sqrt{Q(\xi) + iS''_{n-1}(\xi)}d\xi. \tag{2.19}$$

For our purposes, we only use the approximation S_1:

$$S_1(x) = \pm\int_{x_0}^{x}\sqrt{Q(\xi) + iS''_0(\xi)}d\xi = \pm\int_{x_0}^{x}\sqrt{Q(\xi)}\sqrt{1 \pm i\frac{Q'(\xi)}{2\sqrt{Q(\xi)}Q(\xi)}}d\xi \tag{2.20}$$

$$\approx \int_{x_0}^{x}\left(\pm\sqrt{Q(\xi)} + i\frac{Q'(\xi)}{4\sqrt{Q(\xi)}Q(\xi)}\right)d\xi = \pm\int_{x_0}^{x}\sqrt{Q(\xi)}d\xi + \frac{i}{2}\log\sqrt{Q(x)}, \tag{2.21}$$

up to a constant of integration. Note that we used our assumption 2.17 when expanding the square root and that from the second step we see S_1 is close to S_0, suggesting convergence; more formal proofs are in [23,24]. This implies a solution (also called physical-optics approximation) of the form:

$$\Psi(x) = e^{iS_1(x)} = \frac{C}{Q(x)^{1/4}}\exp\left(\pm i\int_{x_0}^{x}\sqrt{Q(\xi)}d\xi\right). \tag{2.22}$$

If we are treating the radial equation for the quasinormal modes of a black hole, x will be a tortoise coordinate such that the horizon will be at $-\infty$, while spacial infinity will be at ∞, and the potential satisfies our condition 2.17. Now we want to connect our problem of QNMs to a known quantum

mechanics scattering problem. In our case we have no incoming wave from $+\infty$ and at the event horizon waves can only be ingoing into the hole. Therefore, using nomenclature from scattering, we expect transmitted and reflected waves from the interaction with the potential (which has a peak outside the black hole) of similar amplitude. If we calculated the transmission coefficients of this kind of problem we would get a similar result only if the function $-Q(x)$ had one maximum where $Q(x)$ is zero (then, the transmission coefficients are of equal magnitude for the transmitted and reflected wave, each a factor $1/\sqrt{2}$ of the incident one) [24]. This suggests that for normal modes to exist we must have (if the maximum is at x_0) $-Q(x_0) = -Q_0 \approx 0$, which turns out to be our case [21]. In particular, we have $Q_0 \gtrsim 0$, and we call $x_1 < x_2$ the two turning points where $Q(x_-) = Q(x_+) = 0$ (of course it must be $x_1 < x_0 < x_2$). Let us define 3 regions:

$$\text{Region I} \quad x < x_1, \quad \text{Region II} \quad x_1 < x_0 < x_2, \quad \text{Region III} \quad x > x_2. \tag{2.23}$$

In regions I and III (far from the turning points) the solution is of the same form as Eq. 2.22:

$$\Psi_I(x) \approx [Q(x)]^{-1/4} \exp\left(\pm i \int_x^{x_1} (Q(\xi))^{\frac{1}{2}} d\xi\right), \qquad \Psi_{III}(x) \approx Q(x)^{-1/4} \exp\left(\pm i \int_{x_2}^{x} (Q(\xi))^{\frac{1}{2}} d\xi\right). \tag{2.24}$$

Between the turning points we approximate $Q(x)$ with a parabola (this is justified if the turning points are close together):

$$Q(x) \approx Q_0 + \frac{1}{2}\frac{d^2}{dx^2} Q(x)\Big|_{x=x_0} (x - x_0)^2. \tag{2.25}$$

Now we perform the changes of variables:

$$k \coloneqq \frac{1}{2} Q_0'', \quad t \coloneqq (4k)^{\frac{1}{4}} e^{i\frac{\pi}{4}} (x - x_0), \quad \nu + \frac{1}{2} \coloneqq -i \frac{Q_0}{(2Q_0'')^{\frac{1}{2}}}, \tag{2.26}$$

so that we can rewrite our equation (2.14) in the form:

$$\frac{d^2\Psi(t)}{dt^2} + (\nu + \frac{1}{2} - \frac{1}{4}t^2)\Psi(t) = 0. \tag{2.27}$$

The general solution to this equation can be written as

$$\Psi = AD_\nu(t) + BD_{-\nu-1}(it), \tag{2.28}$$

where $D_\alpha(z)$ are parabolic cylinder functions. Having done all this we can use the know asymptotic behaviour of these functions to write [24]:

$$\begin{cases} \Psi \approx & Be^{-3i\pi(\nu+1)/4}(4k)^{-(\nu+1)/4}(x-x_0)^{-(\nu+1)}e^{ik^{1/2}(x-x_0)^2/2} + [A + B(2\pi)^{1/2}e^{-i\nu\pi/2}/\Gamma(\nu+1)] \\ & e^{i\pi\nu/4}(4k)^{\nu/4}(x-x_0)^2 e^{ik^{1/2}(x-x_0)^2/2}, \qquad x \gg x_2, \\ \Psi \approx & Ae^{-3i\pi\nu/4}(4k)^{\nu/4}(x-x_0)^{\nu}e^{-ik^{1/2}(x-x_0)^2/2} + [B - iA(2\pi)^{1/2}e^{-i\pi\nu/2}/\Gamma(-\nu)] \\ & e^{i\pi(\nu+1)/4}(4k)^{-(\nu+1)/4}(x_0-x)^{-(\nu+1)}e^{ik^{1/2}(x-x_0)^2/2}, \qquad x \ll x_1. \end{cases} \tag{2.29}$$

The exponential terms $\exp[-ik^{1/2}(x-x_0)^2/2]$ of both solutions match the wave solutions in (2.24) that respect our boundary conditions, therefore the coefficients of the term $\exp[ik^{1/2}(x-x_0)^2/2]$ must be zero. This is only possible if $B = 0$ and $\Gamma(-\nu) = \infty$ which implies that ν is an integer. But from the definition of ν this also implies:

$$\frac{Q_0}{\sqrt{2Q_0''}} = i(n + \frac{1}{2}), \qquad n = 0, 1, 2, \ldots \tag{2.30}$$

This is a simple condition for the quasinormal modes, as one only needs to compute Q_0 and its second derivative at the extremum point and solve for ω (which is implicitly in Q). For the Schwarzschild black hole it is possible to write a radial eigenvalue problem in ω (withouth any dependence on A_{lm})

with a potential which already satisfies our assumptions, thus this method is extremely useful and simple to implement, and generalizations at higher orders are also possible (see for example [25] which reviews expansions up to the 13th order). Note that in order to satisfy WKB requirements, x must be the tortoise coordinate r_*, and therefore derivatives must be done respect to this variable, and not r. Kerr black holes, as we will see in the next section, present more challenges, and require the discussion of another type of potential, namely one where we have two turning points far apart and $Q(x) > 0$ in between the turning points. To deal with this case, following [24], our strategy is to consider two one-turning-point problems, and then match the solutions we find, meaning we require a single smooth final solution. We start considering one such problem where we can assume the turning point to be at $x = 0$, and we assume our potential has a first order zero at this point, meaning we can write $-Q(x) \sim ax$ (for definiteness we assume $a > 0$, and $-Q(x) < 0$ for $x < 0$, while $-Q(x) > 0$ for $x > 0$). For now, let us neglect the second turning point and assume $Q(x)$ is slowly varying the way to $\pm\infty$ (except of course in the neighbourhood of the turning point). We will then change name to our regions:

$$\text{Region I} \quad x \gg 0, \quad \text{Region II} \quad |x| \ll 1, \quad \text{Region III} \quad x \ll 0. \tag{2.31}$$

We start with region I where the physical-optics approximation holds and our function has the form:

$$\Psi_I = C[-Q(x)]^{-1/4} exp\left[-\int_0^x \sqrt{-Q(\xi)}d\xi\right]. \tag{2.32}$$

In region II our differential equation becomes $\Psi'' = ax\Psi$. We can solve this in terms of Airy functions by making the substitution $t = a^{1/3}x$ and writing the solution

$$\Psi_{II} = D\mathrm{Ai}(t) + E\mathrm{Bi}(t). \tag{2.33}$$

Now, we want to match these solutions, assuming we have some region where our approximations overlap. We will not prove this assumption, for a more formal derivation see [23, 24]. We write our solution in region I for our linear potential

$$\Psi_I \sim C(ax)^{-1/4} \exp\left(\frac{-2\sqrt{a}x^{3/2}}{3}\right). \tag{2.34}$$

Using the asymptotic behaviour of the Airy functions we find

$$\mathrm{Ai}(t) \sim \frac{1}{2\sqrt{\pi}} t^{-1/4} \exp\left(-\frac{2}{3}t^{3/2}\right), \quad \mathrm{Bi}(t) \sim \frac{1}{\sqrt{\pi}} t^{-1/4} \exp\left(\frac{2}{3}t^{3/2}\right), \quad t \to +\infty, \tag{2.35}$$

$$\tag{2.36}$$

meaning

$$\Psi_{II}(x) \sim \frac{1}{\sqrt{\pi}} a^{-1/12} x^{-1/4} \left[\frac{1}{2} D \exp\left(-\frac{2}{3}a^{1/2}x^{3/2}\right) + E \exp\left(\frac{2}{3}a^{1/2}x^{3/2}\right)\right]. \tag{2.37}$$

This implies that $D = 2\sqrt{\pi}a^{-1/6}C$ and $E = 0$. We can then match the two functions in the region where both expressions hold, meaning we must impose that in this region they have the same asymptotic behaviour, obtaining $D = \sqrt{\pi}a^{-1/6}e^{-i\pi/4}$, $E = \sqrt{\pi}a^{-1/6}e^{i\pi/4}$. Now we want to do the matching with our solution in region III, so we can use the asymptotic expansion for Ai and the general expression of Ψ_{III}:

$$\mathrm{Ai}(t) = \frac{1}{\sqrt{\pi}}(-t)^{-1/4} \sin\phi(t), \quad \phi(t) \sim \frac{2}{3}(-t)^{3/2} + \frac{\pi}{4}, \quad t \to -\infty, \tag{2.38}$$

$$\Psi_{III} = F[Q(x)]^{-1/4} \exp\left[+i\int_x^0 \sqrt{Q(\xi)}d\xi\right] + G[Q(x)]^{1/4} \exp\left[-i\int_x^0 \sqrt{Q(\xi)}d\xi\right]. \tag{2.39}$$

This means we have to choose F and G such that Ψ_{II} and Ψ_{III} match in the region they share:

$$\Psi_{III} = \frac{2C}{[Q(x)]^{1/4}} \sin\left[\int_x^0 \sqrt{Q(\xi)}d\xi + \frac{\pi}{4}\right] \sim \frac{2C}{(-ax)^{-1/4}} \sin\left[\frac{2}{3}a^{1/2}(-x)^{3/2} + \frac{\pi}{4}\right], \tag{2.40}$$

$$\Psi_{II} \sim \frac{D}{\sqrt{\pi}} a^{-1/12}(-x)^{-1/4} \sin\left[\frac{2}{3}a^{1/2}(-x)^{3/2} + \frac{\pi}{4}\right]. \tag{2.41}$$

We now have solved the one-turning-point problem, as we have found functions that approximate our solution in all regions. Now, to apply this to our problem with two turning points, we consider two solutions of the kind we just found and match them in the region between the turning points. We then have

$$\Psi_1 = \frac{2C_1}{[Q(x)]^{1/4}} \sin\left[\int_x^{x_+} \sqrt{Q(\xi)}d\xi + \frac{\pi}{4}\right], \quad \Psi_2 = \frac{2C_2}{[Q(x)]^{1/4}} \sin\left[\int_{x_-}^{x} \sqrt{Q(\xi)}d\xi + \frac{\pi}{4}\right]. \tag{2.42}$$

If we rewrite the first one as

$$\frac{2C_1}{[Q(x)]^{1/4}} \sin\left[\int_{x_-}^{x} \sqrt{Q(\xi)}d\xi + \frac{\pi}{4} - \left(\int_{x_-}^{x_+} \sqrt{Q(\xi)}d\xi + \frac{\pi}{2}\right)\right]. \tag{2.43}$$

In order for the two solutions to have the same functional form we must ask for the expression in round brackets to be a multiple of π, moreover, since it is positive, we require that

$$\int_{x_-}^{x_+} \sqrt{Q(\xi)}d\xi = \left(p + \frac{1}{2}\right)\pi, \quad p = 0, 1, 2, \ldots, \tag{2.44}$$

which in quantum mechanics is known as Bohr-Sommerfeld condition.

2.2.1 WKB for Kerr

In this section we want to apply the result we just obtained to the Kerr black hole in the eikonal limit, that is for $l \gg 1$. The procedure is not trivial because we have to simultaneously solve for the angular and radial separation constants ω, A_{lm}, and because we have to deal with complex quantities. We start by writing the radial and angular equations keeping only the leading terms for $l \gg 1$ (and dropping the indices from S^s_{lm} and R^s_{lm}):

$$\frac{1}{\sin\theta}\frac{d}{d\theta}\left[\sin\theta\frac{dS}{d\theta}\right] + \left[a^2\omega^2\cos^2\theta - \frac{m^2}{\sin^2\theta} + A_{lm}\right]S = 0, \qquad \frac{d^2R}{dr_*^2} + \frac{K^2 - \Delta\lambda_{lm}}{(r^2+a^2)^2}R = 0, \tag{2.45}$$

where r_* (the so called tortoise coordinate) and the other quantities we have introduced are:

$$\frac{dr_*}{dr} = \frac{r^2+a^2}{\Delta}, \quad K = -\omega(r^2+a^2) + am, \quad \lambda_{lm} = A_{lm} + a^2\omega^2 - 2am\omega, \quad \Delta = r^2 - 2Mr + a^2. \tag{2.46}$$

We used the fact that $\omega_R = \Re(\omega) \sim \mathcal{O}(l)$, $\omega_I = -\Im(\omega) \sim \mathcal{O}(1)$ (we define ω_I with a minus sign so that it is a positive quantity) and $A_{lm} \sim \mathcal{O}(l^2)$. This comes from the knon results for the Schwarzschild black hole and slowly rotating Kerr black holes (see [6,26]). Note that the equations no longer depend on s. Our strategy to solve the problem is the following: first we solve the problem for only real separation constants, then we consider the imaginary parts as perturbations.

We start with the angular equation, which we rewrite as

$$\frac{d^2S}{dx^2} + V^\theta S = 0, \quad x = \log\left(\tan\frac{\theta}{2}\right), \quad dx = \csc\theta d\theta, \quad V^\theta = a^2\omega^2\cos^2\theta\sin^2\theta - m^2 + A_{lm}\sin^2\theta. \tag{2.47}$$

The variable x acts as a tortoise coordinate: as $\theta \to 0, \pi$, then $x \to \pm\infty$. If we look at the potential written in this form, it is clear that for $m \neq 0$ the function S must go to 0 (meaning waves do not propagate) as $x \to \pm\infty$ ($\theta \to 0, \pi$), while for $m = 0$, S must tend to a constant (not necessarily 0).

We start considering a real frequency $\omega = \omega_R$, and, since ω_R is real, then $A_{lm}(\omega_R)$ must be real too, and we call it $A_{lm}(\omega_R) \equiv A^R_{lm}$. Now we want to understand how this potential is shaped: at the boundary ($\theta = 0, \pi$) the potential is $V^\theta = -m^2$, independent of $A^R_{lm}(\omega_R)$, which means that the solutions to Eq. 2.47 must be decaying exponentially. We are looking for wave-like solutions, which are only possible if $V^\theta > 0$ in some region. Looking at the definition of V^θ we can have two cases: if $A^R_{lm} \geq a^2\omega^2$ the potential has one maximum at $\theta = \pi/2$, while if $A^R_{lm} < a^2\omega^2$ it has two identical maxima, located symmetrically about $\pi/2$. It turns out that solutions where there is some region with $V_\theta > 0$ are of the first kind [6]. The potential in this form is now suited for a WKB analysis, but

we need to check for the condition 2.17 before applying our results. What need to be satisfied is the following:

$$\left|\frac{1}{\sqrt{V^\theta}}\frac{dV^\theta}{d\theta}\right| \ll |V^\theta|. \tag{2.48}$$

Empirically it can be shown that this is true everywhere except the points where $V^\theta = 0$, the so called turning points, see [6]. We solve $V^\theta = 0$ and find the turning points to be:

$$sin^2\theta_\pm = \frac{2m^2}{A_{lm} + a^2\omega_{lm}^2 \mp \sqrt{(A_{lm} + a^2\omega_{lm}^2)^2 + 4m^2}}, \tag{2.49}$$

where we only kept the physical solution. In order to fix notation, we assume $0 < \theta_- < \pi/2$, which implies $\theta_+ = \pi - \theta_-$; we will call $x_\pm$ the corresponding points in the x coordinate. Now we use our WKB result for the two-turning-point problem to write the solution of the wave equation in the region $x_- < x < x_+$. Using 2.39, we obtain:

$$S(x) = \frac{a_+ e^{i\int_0^x dx'\sqrt{V^\theta(x')}} + a_- e^{-i\int_0^x dx'\sqrt{V^\theta(x')}}}{[V^\theta(x)]^{1/4}}, \tag{2.50}$$

where $a_\pm$ are constant to be fixed by the boundary conditions. Similarly we can find solutions in the other regions (we apply 2.32):

$$S(x) = \frac{c_+ e^{-\int_{x_+}^x dx'\sqrt{-V^\theta(x')}}}{[V^\theta(x)]^{1/4}}, \quad \text{for } x > x_+ \quad \text{and} \quad S(x) = \frac{c_- e^{-\int_x^{x_-} dx'\sqrt{-V^\theta(x')}}}{[V^\theta(x)]^{1/4}}, \quad \text{for } x < x_-. \tag{2.51}$$

At the turning points we find solutions using $V^\theta(x \sim x_\pm) \propto x - x_\pm$ (our linear approximation of the potential). Then, as we have already seen, the matching of the solutions lead to this quantization condition 2.44, which in this case reads as:

$$\int_{\theta_-}^{\theta_+} d\theta \sqrt{a^2\omega_R^2\cos^2\theta - \frac{m^2}{\sin^2\theta} + A_{lm}^R} = (L - |m|)\pi, \tag{2.52}$$

where set $n = l - |m|$ in 2.44 and defined $L \equiv l + 1/2$.

It is now useful to define some new quantities:

$$\mu \equiv \frac{m}{L}, \quad \alpha_R(a,\mu) \equiv \frac{A_{lm}^R}{L^2}, \quad \Omega_R(a,\mu) \equiv \frac{\omega_R}{L}, \tag{2.53}$$

which are all $O(1)$ in the expansion in L. We can then rewrite our integral and its limits of integration as

$$\sin^2\theta_\pm = \frac{2\mu^2}{\alpha + a^2\Omega^2 \mp \sqrt{(\alpha + a^2\Omega_R^2)^2 + 4\mu^2}} \qquad \int_{\theta_-}^{\theta_+} d\theta \sqrt{\alpha_R - \frac{\mu^2}{\sin^2\theta} + a^2\Omega^2\cos^2\theta} = (1 - |\mu|)\pi. \tag{2.54}$$

We now want to express α_R as function of μ and Ω_R, this way we effectively decouple the angular problem from the radial one. The exact expression involves elliptic integrals, but in the case of $a\Omega_R$ small we obtain a pretty simple relation (the proof of this is quite lengthy and can be found in [6]), which reads:

$$\alpha_R \approx 1 - \frac{a^2\Omega_R^2}{2}(1 - \mu^2). \tag{2.55}$$

We make a check on our approximation for α_R by comparing this result with the Schwarzschild case, in which $A_{lm}^{Schw} = l(l+1) - s(s+1)$, which means that our approximation is correct up to corrections of order $O(1/L^2)$. It turns out (as shown in [6]) that it is a very good approximation in the case of highly spinning black holes too, so let us give a little insight on why it works so well. We consider corotating modes (m positive and large, or $\mu \approx 1$), which, as they have the highest frequencies, are our

"worst case scenario" for the magnitude of the parameter $a\Omega_R$. If we assume ω_R to be a monotonically increasing function of a, and $\omega_R^{lm}(a) \leq \omega_R^{lm}(a=M) = m\Omega_H^{a=1} = \frac{m}{2M}$, where the upper bound is found using the fact that the low-overtone frequencies, for $m > 0$, approach $m\Omega_H$ in the extremal regime (we will explore this feature in greater detail in the next chapter), and we defined $\Omega_H \equiv \frac{a}{2Mr_+}$ the horizon frequency of the black hole. Then, our bound can be rewritten as $a\Omega_R \leq (\mu/2)(a/M) \leq 1/2$, and even for $a\Omega_R = 1/2$ the relative accuracy of our approximation 2.55 can be found numerically to be 0.2 % [6].

Now, having obtained a manageable expression for $\alpha_R = A_{lm}^R$, we proceed with our discussion of the WKB approximation taking into account the imaginary part of A_{lm}. We work in the hypothesis of $\omega_I \ll \omega_R$, thus allowing us to treat A_{lm}^I, as a perturbation in the angular equation. We apply perturbation theory from quantum mechanics (see for example [23]) to our angular equation, finding at first order of correction:

$$A_{lm}^I = -2a^2\omega_R\omega_I\langle\cos^2\theta\rangle, \quad \langle\cos^2\theta\rangle = \frac{\int\cos^2\theta|S|^2\sin\theta d\theta}{\int|S|^2\sin\theta d\theta} = \frac{\int_{\theta_-}^{\theta_+}\frac{\cos^2\theta}{\sqrt{a^2\omega_R^2\cos^2\theta-\frac{m^2}{\sin^2\theta}+A_{lm}^R}}d\theta}{\int_{\theta_-}^{\theta_+}\frac{1}{\sqrt{a^2\omega_R^2\cos^2\theta-\frac{m^2}{\sin^2\theta}+A_{lm}^R}}d\theta}. \tag{2.56}$$

We can simplify this expression: taking the derivative of Eq. 2.52 with respect to $z \equiv a\omega_R$, and treating $A_{lm} = A_{lm}(z)$ we can rewrite Eq. 2.56 as

$$\langle\cos^2\theta\rangle = -\frac{1}{2z}\frac{\partial A_{lm}^R(z)}{\partial z}\bigg|_{z=a\omega_R}, \qquad A_{lm}^I = a\omega_I\left[\frac{\partial A_{lm}^R(z)}{\partial z}\right]_{z=a\omega_R}. \tag{2.57}$$

We have then obtained an expression for $A_{lm} = A_{lm}^R + iA_{lm}^I$; in particular, we can rewrite what we obtained before in Eq. 2.55 (defining $\Omega = \omega/L$) as

$$A_{lm} \approx L^2 - \frac{a^2\omega^2}{2}\left[1-\frac{m^2}{L^2}\right], \qquad \text{or} \qquad \alpha \approx 1 - \frac{a^2\Omega^2}{2}(1-\mu^2). \tag{2.58}$$

We have successfully obtained an expression for the angular separation constant as a function of ω, meaning we can decouple the radial equation and determine the quasinormal frequencies. Similarly as we did before, we start by rewriting the radial equation as a bound state problem

$$\frac{d^2R}{dr_*^2} + V^rR = 0, \quad V^r(r,\omega) = \frac{[\omega(r^2+a^2)-ma]^2 - \Delta[A_{lm}(a\omega)+a^2\omega^2-2ma\omega]}{(r^2+a^2)^2}. \tag{2.59}$$

We notice that V^r is an analytic function of ω and it is real-valued when ω is real. This potential is ready for a WKB analysis, however this time we invoke the results from the previous section for very close turning points. In general we write our radial solution far from the extremum of the potential as

$$R = b_+e^{i\int^{r_*}\sqrt{V^r(r_*')}dr_*'} + b_-e^{-i\int^{r_*}\sqrt{V^r(r_*')}dr_*'}, \tag{2.60}$$

where we used 2.24. However, in order to satisfy the boundary conditions, we will actually have

$$R = b_+e^{i\int^{r_*}\sqrt{V^r(r_*')}dr_*'}, \quad \text{as } r_* \to -\infty, \qquad R = b_-e^{-i\int^{r_*}\sqrt{V^r(r_*')}dr_*'}, \quad \text{as} \quad r_* \to +\infty.$$

Now, we want to invoke Eq. 2.30. Since for a real frequency everything on the left-hand side is real, the following conditions must hold (the second equality comes from the definition of r_0 as the maximum of the potential):

$$V^r(r_0,\omega_R) = \frac{\partial V^r}{\partial r}\bigg|_{(r_0,\omega_R)} = 0, \tag{2.61}$$

which, after some work, can be expressed as

$$\Omega_R = \frac{\mu a}{r_0^2+a^2} \pm \frac{\sqrt{\Delta(r_0)}}{r_0^2+a^2}\beta(a\Omega_R), \quad 0 = \frac{\partial}{\partial r}\left[\frac{\Omega_R(r^2+a^2)-\mu a}{\sqrt{\Delta(r)}}\right]_{r=r_0}. \tag{2.62}$$

We defined

$$\beta(z) = \sqrt{\alpha(z) + z^2 - 2\mu z} \approx \sqrt{1 + \frac{z^2}{2} - 2\mu z + \frac{\mu^2 z^2}{2}}, \tag{2.63}$$

and we used the fact that for $r > r_+$, $(r^2 + a^2)^2/\Delta$ is a monotonically increasing function, as well as the fact that the quantity in square brackets in Eq. 2.62 is never zero when $V^r = 0$. Note that we lose the dependence on the index n which would represent the overtone number. We will see later that we recover the dependence on n only in the imaginary part of the frequency. In order to determine $\omega_R = \Omega_R L$, we need to solve both equations 2.62, however the calculations are different for $m = 0$ and $m \neq 0$. Let us start with $m \neq 0$. The first step is to use the second one of Eq. 2.62 to express Ω_R as a function of r_0 as

$$\Omega_R = \frac{(M - r_0)\mu a}{(r_0 - 3M)r_0^2 + (r_0 + M)a^2}, \tag{2.64}$$

and use this and the first of Eq. 2.62 to eliminate r_0. If we use the approximate formula for $\beta(z)$, r_0 is found as the root of the polynomial (defining $x = r_0/M$):

$$2x^4(x-3)^2 + 4x^2[(1-\mu^2)x^2 - 2x - 3(1-\mu^2)](a/M)^2 + (1-\mu^2)[(2-\mu^2)x^2 + 2(2+\mu^2)x + (2-\mu^2)](a/M)^4. \tag{2.65}$$

For each $(\mu,\, a/M)$ there are in general two real roots for x, corresponding to a positive or a negative Ω_R. We saw at the end of chapter 1 that this is to be expected and that we do not lose any information by only consider one of the two solutions (to any solution $(\omega_{lm}, {}_sA_{lm})$ corresponds another solution $(-\bar{\omega}_{l-m}, {}_s\bar{A}_{l-m})$). Thus, we can assume $\Omega_R > 0$. If instead $m = 0$, both numerator and denominator of 2.64 vanish and the procedure we just outlined does not work. In this case, we directly require

$$(r_p - 3M)r_p^2 + (r_p + M)a^2 = 0. \tag{2.66}$$

r_p can be found in closed form and inserted in Eq. 2.62 to obtain:

$$\Omega_R(a, \mu = 0) = \pm\frac{1}{2}\frac{\pi\sqrt{\Delta(r_p)}}{(r_p^2 + a^2)\mathrm{EllipE}[a^2\Delta(r_p)/(r_p^2 + a^2)^2]}, \tag{2.67}$$

where EllipE is an elliptic integral of the second kind (see [6] for details on the calculation). What is left is to calculate ω_I, which we can find using our result 2.30: we expand the left-hand side at first order in ω_I to obtain

$$\omega_I = -(n + \frac{1}{2})\frac{\sqrt{2\left(\frac{d^2V^r}{dr_*^2}\right)_{r_0,\omega_R}}}{\left(\frac{\partial V^r}{\partial\omega}\right)_{r_0,\omega_R}}, \tag{2.68}$$

where n is the overtone number. Recalling that V^r also depends on ω both explicitly and through A_{lm}, we use our approximate formula for α to obtain a final solution to our problem

$$\omega_I = -\left(n + \frac{1}{2}\right)\frac{\Delta(r_0)\sqrt{4(6r_0^2\Omega_R^2 - 1) + 2a^2\Omega_R^2(3 - \mu^2)}}{2r_0^4\Omega_R - 4aMr_0\mu + a^2r_0\Omega_R[r_0(3 - \mu^2) + 2M(1 + \mu^2)] + a^2\Omega_R(1 - \mu^2)}. \tag{2.69}$$

We have then obtained analytical expressions for the real and imaginary part of our frequencies. Note that the dependence on the overtone number n is only in the imaginary part and that there is no dependence on the spin weight s. In the next sections we will compare these results with the ones obtained with the continued fraction method, in order to determine the accuracy of this approximation.

2.3 Numerical results

2.3.1 Schwarzschild

We now begin calculating the quasinormal frequencies with the methods presented before. The first case we analyze is the Schwarzschild black hole, where we set the rotational parameter $a = J/M = 0$ (J being the angular momentum of the black hole, M its mass). In this case the radial and angular equations decouple, allowing us to directly calculate the the angular separation constant analytically,

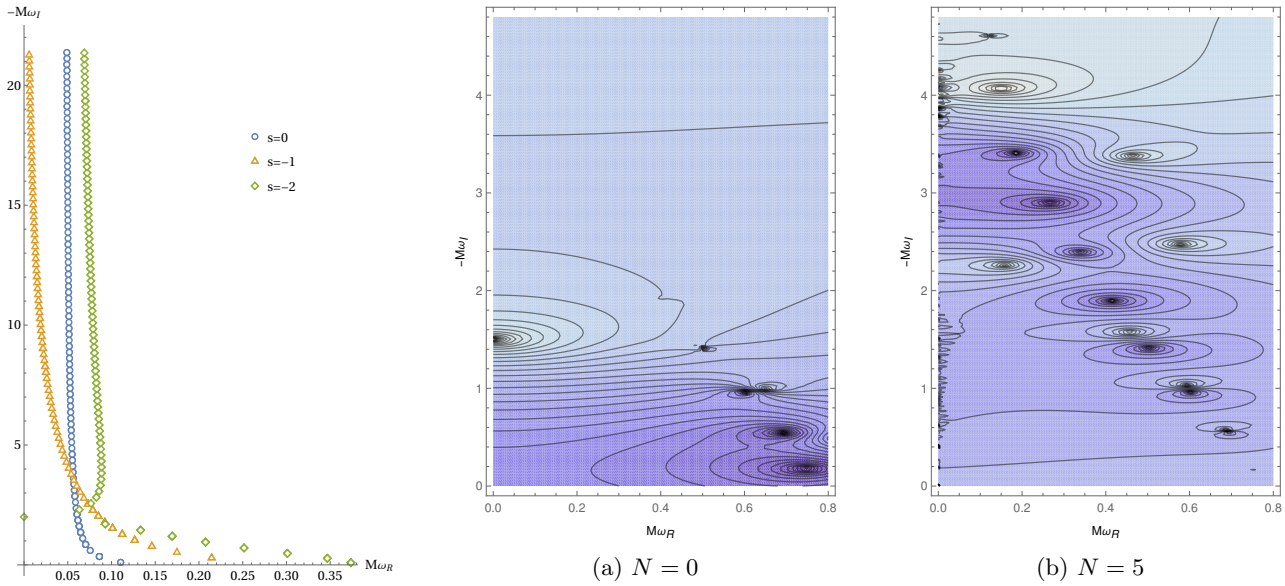

(a) $N = 0$ (b) $N = 5$

Figure 2.1: From the left: modes for the Schwarzschild black hole for different values of the spin weight s and $l = |s|$, plots of the (logarithm of the absolute value of) the continued fraction at different number of inversions (N).

its value being $A_{lm} = l(l+1) - s(s+1)$, where s is the spin weight [19]. To compute the quasinormal modes we calculate the continued fractions 2.12 truncated at a sufficiently high term guaranteeing convergence up to a certain threshold. This might not be the same for all modes, in fact we observe that for higher overtones the number of terms in the continued fraction needs to be increased significantly in order to guarantee a stable numerical result. Another important observation is that even though the roots of the continued fraction do not vary by inverting it, its topology changes significantly. For example in panels (a) and (b) in Fig. 2.1 we plot the logarithm of the absolute value of the continued fraction, N being the number of inversions. Quasinormal frequencies, being the zeros of the continued fraction, can be identified as the points where contours cluster. Note that there are both darker and lighter clusters, the former are quasinormal modes, while the latter are poles, which have no physical meaning, as they change position by changing the number of inversions of the continued fractions. One last remark is that the absence of certain modes in either of the panels does not mean that the functions have different zeros, but that with the used precision we cannot distinguish all of the modes. This means it might be easier to find certain roots with a different number of inversions. Usually, the nth overtone is found to be the most stable root of the $n = N$th, inversion of the continued fraction, although this is not always the case. We use the fact that inversions do not change the roots of the continued fraction to test the stability of our results: checking whether we can find the same mode with different inversions is faster than increasing the number of terms in the fraction, and can be a first test in spotting mistakes.

We implement Leaver's method in a `Mathematica` notebook, our code being a modified version of the one found in [5]. The algorithm we use to find the roots of the continued fraction is the non-linear root finding algorithm of `Mathematica`, `FindRoot`. One thing we note is that, particularly for higher overtones, the algorithm is heavily dependent on the initial guess, therefore in order to obtain all QNMs we set a search grid of initial values and test each value against different numbers of inversions of the continued fraction, the spacing of the grid chosen small enough to guarantee to find all modes. Roots found in this way are then used as initial values for the root finding algorithm using a different number of inversions and increasing number of terms in the continued fraction (quasinormal modes must be stable against these tests). In this way we are certain that all the values we find are actually part of the spectrum. As we said before, to find modes further away from the real axis it is necessary to increase the number of terms in the continued fraction. Our results for the Schwarzschild metric are summarized in the panel on the left in Fig. 2.1, where we calculated frequencies for $s = 0, -1, -2$ and $l = |s|$. We find perfect accord with the existing literature, see for example Fig. 5 in [4] or [5]. Note

that we do not plot the negative real axis: in the Schwarzschild case, since we have no dependence on m, the symmetry $\omega_{lm} = -\omega^*_{l-m}$ implies the spectrum is symmetric about the imaginary axis. This will not be the case for other values of the rotational parameter a. We notice by looking at the spectrum for different values of the spin weight s that only gravitational perturbation touch the the imaginary axis, at the so-called algebraically special mode. These modes are extremely interesting and their phenomenology quite rich, but it would take too much space in this thesis, more on these modes in [4, 27]. This mode is also quite difficult to obtain numerically, as we observe that we need a very high number of terms in the continued fraction before it converges. We find a result is in accord with [5], however numerical determination of this mode has been quite problematical and it has been studied in great detail, see for example appendix A in [4]. Another difficulty we notice regards modes close to the imaginary axis, for example electromagnetic modes ($s = -1$) with a large imaginary part require more terms in the continued fraction.

2.3.2 Non-extremal Kerr

We now turn to Kerr black holes. First, we study the non extremal case, meaning we keep the rotational parameter away from the extremal limit $a/M = 1$. We use a method similar to the one employed in the last section: we implement Leaver's method in a `Mathematica` notebook and use the function `FindRoot` to compute the zeros of the continued fraction. However, since the angular and radial equations (Eq. 1.42 and Eq. 1.43) are coupled, we need to solve for both separation constants ω_{lm} and A_{lm} simultaneously. This is done through an iterative process, where we first initialize both quantities with a certain value and then solve one of the continued fractions (Eq. 2.9 or Eq. 2.12) and use the result in the other. We repeat this until there is convergence. Since we are computing these modes for different values of a, starting from $a = 0$ (the Schwarzschild case), we use as initial values the ones we find for the previous value of a, starting from the ones obtained in the last section.

We now present our results: we calculated the first eight overtones for the Kerr black hole with $s = -2$, $l = 2$ and $m = 0, \pm 1, \pm 2$. The choice of these values is not random, as these are the ones that dominate the ringdown of black hole mergers, and thus the most interesting ones from an astrophysical perspective (actually we should add $m \geq 0$, but here we are interested in seeing the features of negative m too) [28, 29]. Our results are summarized in Fig. 2.2 and reproduce the ones obtained for example in Fig. 3 in [19] or [5]. We do not plot the negative real axis, as it would not give any new information. However, unlike the Schwarzschild case, due to the m dependence, there is not perfect symmetry about the imaginary axis. To reconstruct the entire spectrum we proceed as follow: take a mode ω_{lm} such that $\Re(\omega_{lm}) > 0$ and $m > 0$, then the $-m$ branch will have $\Re(\omega_{l-m}) < 0$, however, it exists a mode which has negative real part for positive m and whose $-m$ branch will be the reflection of the lost branch about the imaginary axis (which is represented in the plot). An important observation is that the dependence on m causes a Zeeman-like splitting of the spectrum, with different branches corresponding to different m, see panel (a) in Fig. 2.2.

2.3.3 WKB approximation

We now want to compare our WKB approximation with the results obtained with Leaver's method. Since we have performed an expansion up to the next-to-leading order for ω_R we expect the error to be scaling as $\mathcal{O}(1/L^2)$ ($L = l + 1/2$), while, since we only calculated the leading order for the imaginary part ω_I, we would expect an error of order $\mathcal{O}(1/L)$. In Fig. 2.3 we have represented our results: we used the formulas we obtained in 2.64, 2.67 and 2.69 to calculate the approximate values of the real and imaginary part of the frequency for the fundamental mode at various $\mu = m/L$. We are considering gravitational perturbations, $s = -2$, which are the "worst case scenario", as the WKB approximation does not depend on the spin weight (thus, it should work the best in the scalar case). We plot the relative errors $\delta\omega/\omega$ multiplied by L^2 for both the real and imaginary part of the frequency, where the exact values are obtained with Leaver's method and checked against [30]. The scaled relative error of the real frequency quickly becomes constant as L increases, confirming our prediction. If we look at the relative error of the imaginary frequency, however, we find that it still scales as $1/L^2$, meaning our approximation is even better than what we anticipated. Our results are perfectly in agreement with the literature (see Figs. 6, 8 in [6]).

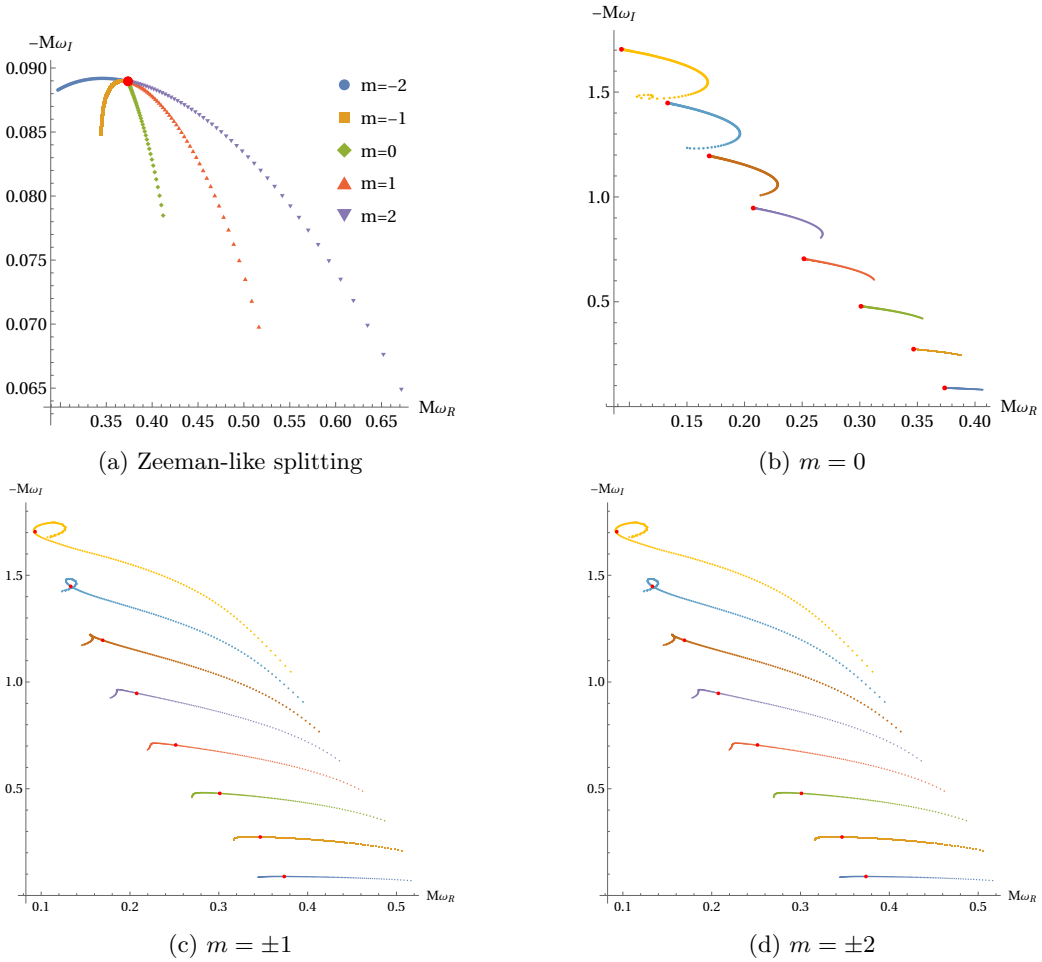

(a) Zeeman-like splitting

(b) $m = 0$

(c) $m = \pm 1$

(d) $m = \pm 2$

Figure 2.2: In panel (a) the fundamental mode of Kerr black hole with $0 \leq a/M \leq 0.9$, $s = -2$, $l = 2$ and $m = 0, \pm 1, \pm 2$. In panels (b)-(d) the first 8 QNMs for Kerr black hole, with $0 \leq a/M \leq 0.9$, $l = 2$ and $m = 0, \pm 1, \pm 2$. The points highlighted in red are the Schwarzschild modes.

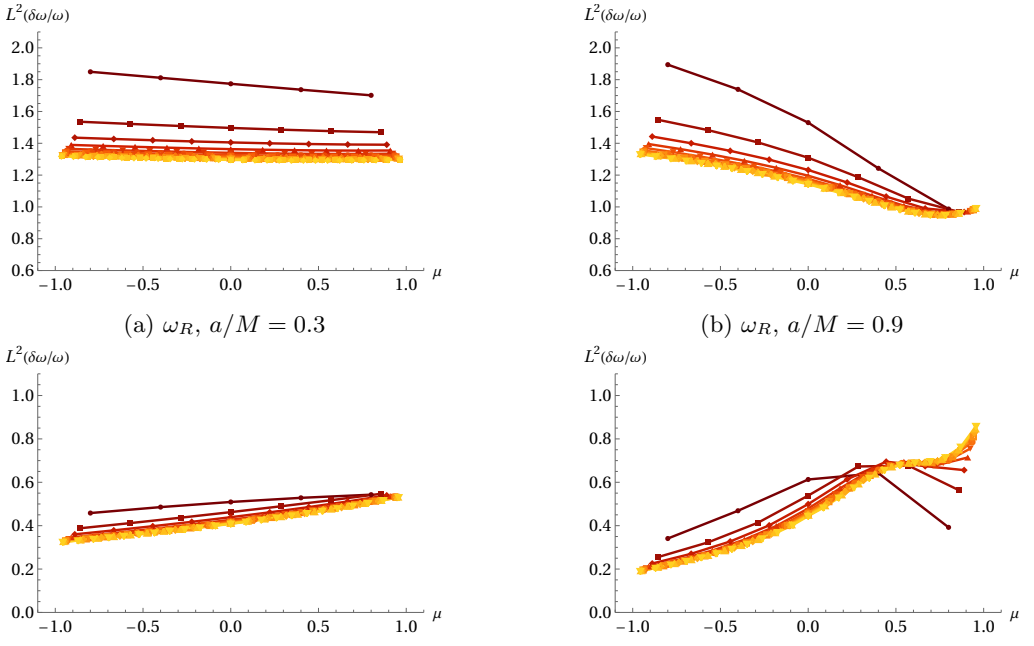

(a) ω_R, $a/M = 0.3$

(b) ω_R, $a/M = 0.9$

(c) ω_I, $a/M = 0.3$

(d) ω_R, $a/M = 0.9$

Figure 2.3: Comparison between WKB approximation and continued fraction method. We plot the relative error $(\delta\omega/\omega)L^2$ for the fundamental gravitational mode as a function of $\mu = m/L$ for different values of $L = l + 1/2$ (l from 2 to 14) and a/M. In each plot the uppermost line (or in any case the darkest one) is $l = 2$, then, $l = 3, 4, \ldots$ going down.

3. Computing QNMs: near-extremal and extremal Kerr

3.1 Near-extremal kerr

3.1.1 Damped modes and zero-damping modes

We now turn our attention to the case of near-extremal Kerr. Here the peculiar characteristics of the spectrum call for a more careful studying of the quasinormal modes. Until now, we have classified modes with the same indices (l, m) by the overtone number n, which labeled frequencies based on the magnitude of their imaginary part. As we approach extremality, however, we have certain values of (l, m) for which the spectrum bifurcates, and this is not possible anymore. We distinguish two types of QNM: damped modes (DM) and zero-damping modes (ZDM). The former maintain a nonzero imaginary part even in the extremal limit, while the latter all tend to a common value $M\omega \to m/2$, which is purely real (hence the name zero-damping). ZDMa are also called synchronous frequencies and exist for all $(l, m \geq 0)$, while DMs exist for any $(l, m \leq 0)$. There are no ZDMs theoretically predicted for $m < 0$ as discussed in [7], while for $m \geq 0$ there are situations in which the two types of modes can coexist. The boundary between the values of l and m where the two types of modes coexist is called phase boundary (see Fig. 3.1).

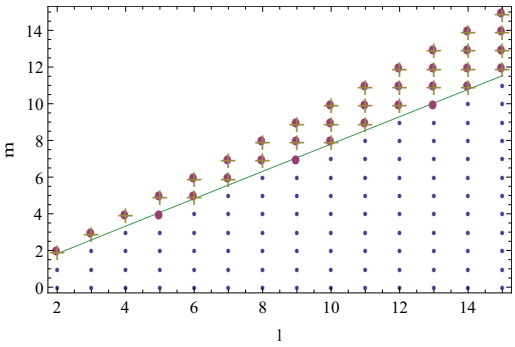

Figure 3.1: Taken from [7]. Phase diagram for the existance of DM and ZDM. Large purple dots ($s = -2$) and gold crosses ($s = 0$) correspond to (l, m) pairs with only ZDMs, while smaller blue dots correspond to (l, m) pairs with both ZDMs and DMs. The green line is the phase boundary computed using the eikonal approximation and the WKB method.

3.1.2 WKB for near-extremal Kerr

We want to apply our WKB technique the nearly extremal limit as $a \to 1$, following what is outlined in [7]. We give a very brief idea on how the WKB method gives us insight on the difference between DMs and ZDMs, for a more in depth description see [6,7]. We start rewriting the radial potential (Eq. 2.59) in the extremal limit (we set for brevity $r_+ = r_- = M = 1$) as

$$V^r = L^2 \frac{(r-1)^2}{(r^2+1)^2} \left[\frac{(r+1)^2}{4}\mu^2 - \alpha + \frac{3}{4}\mu^2 \right], \tag{3.1}$$

where $\mu = m/L$, $\alpha = A_{lm}/L^2$, $L = l + 1/2$. As we approach this limit, for some $\mu > 0$, the peak of the potential r_0 approaches the horizon. This only happens above some critical value μ_c. What we want to show here is that μ_c can be used to define the boundary in the phase diagram in Fig. 3.1. We could show that for values below μ_c the peak of the potential stays outside the horizon even as $a \to 1$, and the horizon is another extremum point. Above μ_c in the extremal limit there is only one peak at the horizon. By this definition of μ_c, we write the condition $\mu > \mu_c$ as

$$\frac{(r+1)^2}{4}\mu^2 - \alpha + \frac{3}{4}\mu^2 > 0 \quad \text{for } r = 1. \tag{3.2}$$

It is useful to rewrite this by defining the quantity $\mathcal{F}_0 = L\sqrt{\frac{7\mu^2}{4} - \alpha|_{\Omega_R = \mu/2}}$ ($\Omega_R = \Re(\omega)/L$). Then, our condition is the simple $\mathcal{F}_0^2 > 0$. Using our approximation of A_{lm} 2.55 we find $\mu_c \approx 0.744$. We can write the radial coordinate of the horizon as $r_+ = 1 + \sqrt{2\epsilon}$ where we expanded up to first order in $\epsilon = 1 - a \ll 1$. Now, consider the case $\mathcal{F}_0^2 > 0$: if we assume that r_0 approaches the horizon with a similar behaviour, that is writing $r_0 = 1 + c\sqrt{\epsilon}$, with c to be determined, we obtain, by solving the WKB equations for r_0 and ω (Eq. 2.65, 2.64, 2.69) [7]:

$$r_0 = 1 - \frac{m\sqrt{2\epsilon}}{\mathcal{F}_0}, \qquad \omega = \left(\frac{m}{2} - \mathcal{F}_0\sqrt{\frac{\epsilon}{2}}\right) - i\left(n + \frac{1}{2}\right)\sqrt{\frac{\epsilon}{2}}. \tag{3.3}$$

That is, for $\mathcal{F}_0^2 > 0$, modes have a vanishing imaginary part, and the only peak is at the horizon: only ZDMs exist. If $\mathcal{F}_0^2 < 0$, the WKB approximation predicts DMs, and the potential peak is outside of the horizon. To explain how ZDMs are allowed too when $\mathcal{F}_0^2 < 0$, we would need a more in depth analysis of the near-to-extremal solutions of Teukolsky equation. In this work we will not review these arguments, however, these calculations and more on the geometrical interpretation of quasinormal modes are found in [6, 7].

3.1.3 Numerical results

In this section, as we did in the non-extremal case, we focus our analysis on the gravitational modes with $l = 2$, particularly the ones with $m \geq 0$. Now, let us consider a case in which both DM and ZDM exist, for example in Fig. 3.2 we report our results for the case of gravitational perturbation $l = 2$ and $m = 1$. We computed these modes in the same way as in the non-extremal case (see Sec. 2.3.2), using a `Mathematica` notebook to implement Leaver's continued fraction method. Lines start at $a/M = 0.9$ and end at $a/M = 0.99999$, and points are calculated for logarithmically spaced values of a. In the numerical analysis we notice that, as we approach the extremal limit, it is crucial to reduce the spacing between different values of a in order to proceed as before using the last found value of ω_{lm} as a starting guess for the new a. One particular problem was the mode D1 in Fig. 3.2,which required the highest number of inversions to converge to its correct value in the extremal limit. Our results are in great agreement with Fig. 8 of [7]. Looking at Fig. 3.2, and comparing it with Fig. 2.2 we can see that, as we approach extremality, the single branch that we have in the case of Schwarzschild and slowly rotating Kerr black holes bifurcates into two different branches. This means that for some value of the rotational parameter a the spectrum bifurcates.

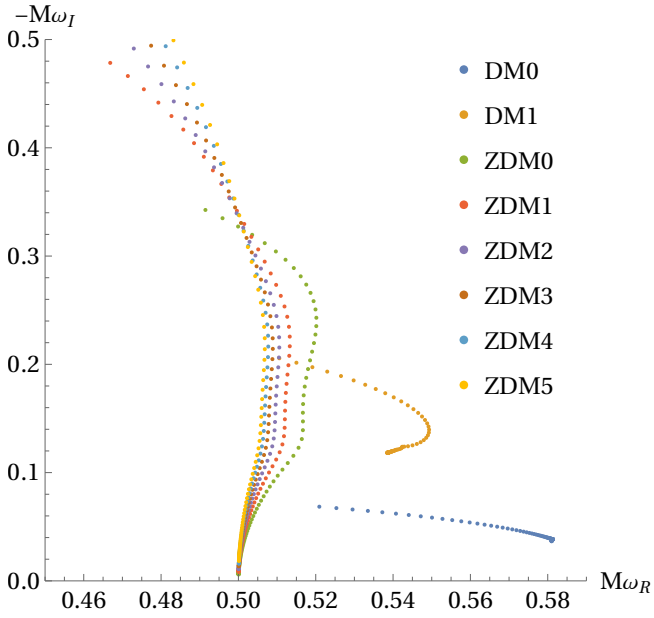

Figure 3.2: QNMs for $(s = -2, l = 2, m = 1)$. Lines start from $a/M = 0.9$ and end at $a/M = 0.99999$ with logarithmically spaced points. Some lines in the upper part of the plot have been truncated to better see the other modes.

In order to better understand what happens at this bifurcation, we study contour plots of the continued fraction, a method which allows us to observe multiple QNMs for a fixed value of the rotational parameter. We plot the value of the continued fraction in a region of the frequency complex plane (for each point we have to calculate its coupled angular separation constant A_{lm}) for different values of m and a in Fig. 3.3. These results are in accord with accord Fig. 7 of [7]. We start from the case $m = 0$. In panel (a) of Fig. 3.3 we can see a clear bifurcation of the spectrum when the angular parameter is $a/M = 0.998$. On the right branch we see a high number of DMs (11) with $\Re(\omega) > 0$, a twelfth one on the imaginary axis and also some of the symmetric modes with $\Re(\omega) < 0$. The identification of the twelfth mode as a DM comes from an analysis at a higher a, as from this graph we cannot predict whether the imaginary part of that mode will decrease. The ZDMs are clustered on the imaginary axis (the all tend to $M\omega \to m/2 = 0$). Panel (d) is a zoom on the first three ZDMs; once again we stress that it is important not to confuse QNMs with the poles in the function. The case of $m = 1$ (panels (b) and (e) in Fig. 3.3) is close to the phase boundary (for $m = 2$ no DMs exist), and it shows a clear spectrum bifurcation. By increasing the angular momentum from $a = 0.99$ to $a = 0.999$ we see that the first ZDM has a lower imaginary part than the highest DM, meaning we have crossed the bifurcation point. In this case we only have two DMs, thus we can re-number ZDM with a new overtone index $n' = n - 2$ (the third QNM will then be the first ZDM, and so on). This case is also interesting because these values of the rotational parameter are not far from what can be reached

in models of astrophysical black holes (for example [31] puts a limit on the rotational parameter of a rotating black hole which swallows matter and radiation from an accretion disc of $a/M \lesssim 0.998$, while [32] puts a limit even closer to extremality). Finally, for of $m = 2$ (panels (c) and (f) in Fig. 3.3), we only have ZDMs, and we can see that, approaching extremality, all frequencies tend to the predicted value $M\omega_{lm} \to m/2 = 1$ (careful not to be confused with poles, the right branch clusters are not QNMs).

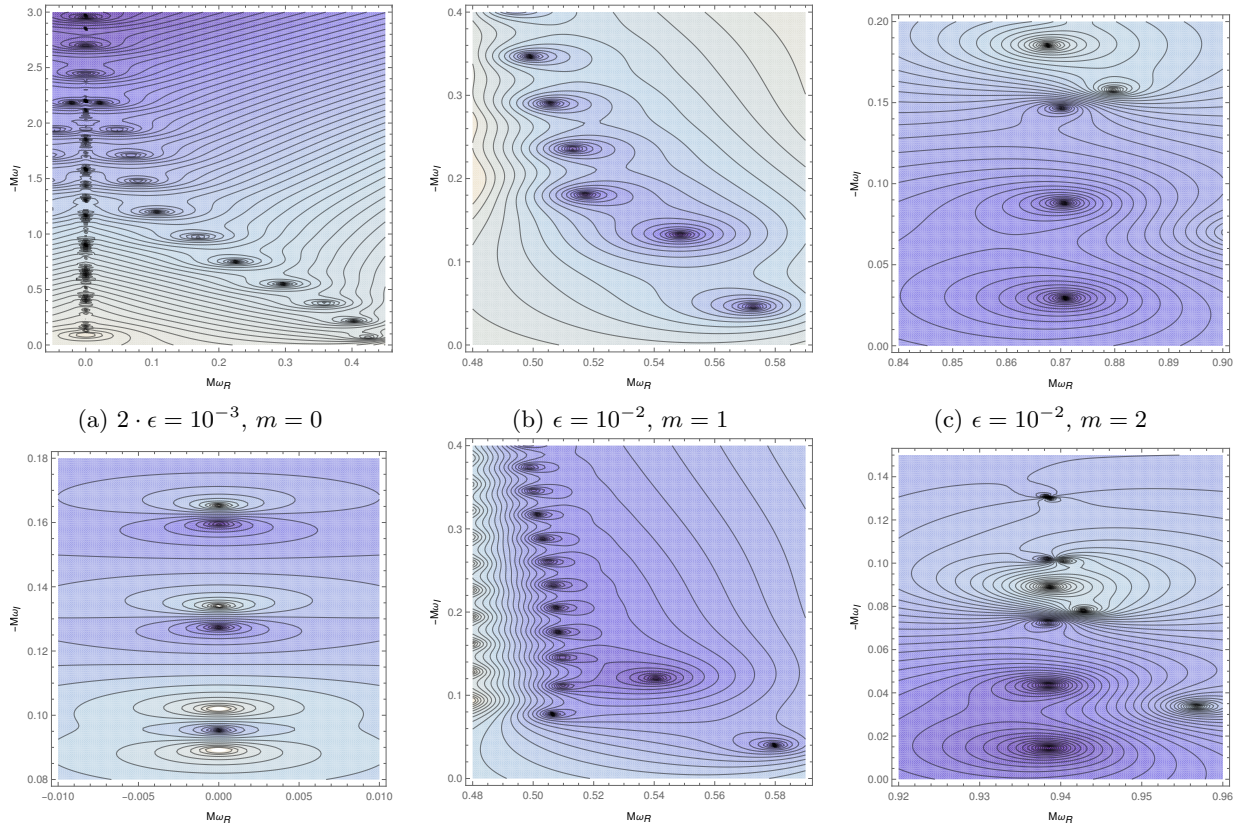

(a) $2 \cdot \epsilon = 10^{-3}$, $m = 0$ (b) $\epsilon = 10^{-2}$, $m = 1$ (c) $\epsilon = 10^{-2}$, $m = 2$

(d) $\epsilon = 2 \cdot 10^{-3}$, $m = 0$ (e) $\epsilon = 2 \cdot 10^{-3}$, $m = 1$ (f) $\epsilon = 2 \cdot 10^{-3}$, $m = 2$

Figure 3.3: Contour plots of Leaver's continued fraction varying m and $\epsilon \equiv 1 - a/M$.

3.2 Extremal Kerr

3.2.1 The extremal case: a modified continued fraction method

We now want to explore the extremal case in which $a/M = 1$. In this regime Leaver's method cannot be employed, but it is still possible to tackle this problem and calculate QNM frequencies with a continued fraction method, though the expansion is different than the one proposed by Leaver. In this section we describe a method, developed by Richartz in [33], which allows us to calculate QNMs for the extremal Kerr black hole (though not in the case $M\omega = m/2$ of synchronous frequencies). We want to see if by assuming $a/M = 1$ from the beginning we obtain the same result as we would by taking the limit of the near-extremal case, and thus if Leaver's method can approximate the modes of the strictly extremal Kerr black hole.

First, we proceed as in the non-extremal case, solving the radial equation 1.43 in the asymptotic limits of $r \to M$ and $r \to \infty$. We can find analytical solutions in both cases, and after imposing our boundary conditions, only ingoing modes at the horizon and only outgoing modes at infinity, we are left with (in our geometrized units, in the extremal case, $r_- = r_+ = M$):

$$R(r) \sim e^{\frac{J_0}{r-M}}(r-M)^{J_1}, \quad \text{as } r \to M, \qquad R(r) \sim r^{J_1+J_2}e^{i\omega r}, \quad \text{as } r \to \infty, \tag{3.4}$$

where we defined $J_0 = iM(2M\omega - m)$, $J_1 = -2s - 2iM\omega$ and $J_2 = -1 + 4iM\omega$. Here is the first difference from Leaver: instead of expanding the radial solution around the event horizon, we do it

around the non-singular point $r = 2M$, obtaining

$$R(r) = e^{i\omega r} e^{\frac{J_0}{r-M}} (r-M)^{J_1} r^{J_2} \sum_{n=0}^{\infty} a_n \left(\frac{r-2M}{r}\right)^n . \tag{3.5}$$

After plugging this back in the radial equation we find a recurrence relation the coefficients must satisfy, though it is more complicated than the Leaver case:

$$\alpha_1 a_2 + \beta_1 a_1 + \gamma_1 a_0 = 0, \tag{3.6}$$
$$\alpha_2 a_3 + \beta_2 a_2 + \gamma_2 a_1 + \delta_2 a_0 = 0, \tag{3.7}$$
$$\alpha_n a_{n+1} + \beta_n a_n + \gamma_n a_{n-1} + \delta_n a_{n-2} + \epsilon_n a_{n-3} = 0. \tag{3.8}$$

The coefficients for the five-term recurrence relation (3.8) are given explicitly by

$$\begin{cases} \alpha_n &= n^2 + n, \\ \beta_n &= P_1 n, \\ \gamma_n &= -2n^2 + P_2 n + P_3, \\ \delta_n &= P_4 n + P_5, \\ \epsilon_n &= n^2 + P_6 n + P_7, \end{cases} \quad \text{where} \quad \begin{cases} P_1 &= 4(im - iM\omega - s), \\ P_2 &= 2(1 - 4im + 16iM\omega), \\ P_3 &= -2[1 + 2s + 2A_{lm} + 2iM\omega(4 + 23iM\omega), \\ & \quad -2im(1 + 6iM\omega)], \\ P_4 &= 4(im - iM\omega + s), \\ P_5 &= -4(im - iM\omega + s)(1 + 4iM\omega), \\ P_6 &= -3 - 8iM\omega, \\ P_7 &= 2[1 + 6iM\omega - 8(M\omega)^2]. \end{cases} \tag{3.9}$$

We now want to prove the series' convergence, through the ratio test. We study a_{n+1}/a_n as $n \to \infty$ and use our recurrence relation to find four different asymptotic solutions:

$$\mathcal{R}^I_{\pm} = \frac{a_{n+1}}{a_n} = 1 \pm 2\sqrt{\frac{-iM\omega}{n}} + \mathcal{O}(n^{-1}), \quad \mathcal{R}^{II}_{\pm} = \frac{a_{n+1}}{n} = -1 \pm \sqrt{\frac{-J_0}{Mn}} + \mathcal{O}(n^{-1}). \tag{3.10}$$

$|a_{n+1}/a_n| \to 1$ in all four cases, therefore our sum is convergent as long as $M < r < \infty$. However, what we need is convergence also for $r = M$ and $r = \infty$, as in order to have QNMs we need to impose boundary conditions at these points. To gain more information on the convergence of our series we use Raabe's test. Let us define

$$\rho_n \equiv n \left[\frac{a_n}{a_{n+1}} \left(\frac{r-2M}{r}\right)^{-1} - 1 \right], \tag{3.11}$$

then the test states that series converges if $\rho > 1$, it diverges if $\rho < 1$, and we have no additional information if $\rho = 1$. In our case, by studying the cases $r = M$ and $r \to \infty$ we see that the only acceptable solutions are R^I_- and R^{II}_+. This does not work when $iM\omega$ or J_0 are positive real numbers, as in the case the coefficient of the term $\propto n^{-1/2}$ in our ratios becomes purely imaginary, or if $M\omega = m/2$, in which case $J_0 = 0$. In these hypothesis, then, our series converges. The relation 3.8 has four independent solutions (each one of them giving one of the four asymptotic ration behaviour mentioned above), while Eq. 3.7 and Eq. 3.6 remove two degrees of freedom. Another way of seeing this (which is useful for the computation of the continued fraction) is to perform two Gaussian eliminations in order to transform our three recurrence relations in a single three-term relation

$$\alpha''_n a_{n+1} + \beta''_n a_n + \gamma''_n a_{n-1} = 0, \quad n \geq 1, \tag{3.12}$$

where the new coefficients are obtained recursively from the original ones as:

$$\begin{cases} \alpha'_1 = \alpha_1,\ \beta'_1 = \beta_1,\ \gamma'_1 = \gamma_1, \\ \alpha'_2 = \alpha_2,\ \beta'_2 = \beta_2,\ \gamma'_2 = \gamma_2,\ \delta'_2 = \delta_2, \\ \epsilon'_n = 0,\ \alpha'_n = \alpha_n,\ \beta'_n = \beta_n - \frac{\epsilon_n}{\delta'_{n-1}}\alpha'_{n-1},\ n \geq 3 \\ \gamma'_n = \gamma_n - \frac{\epsilon_n}{\delta'_{n-1}}\beta'_{n-1}, \delta'_n = \delta_n - \frac{\epsilon_n}{\delta'_{n-1}}\gamma'_{n-1},\ n \geq 3 \end{cases} \quad \begin{cases} \alpha''_1 = \alpha'_1,\ \beta''_1 = \beta'_1,\ \gamma''_1 = \gamma'_1, \\ \alpha''_n = \alpha'_n,\ \beta''_n = \beta'_n - \frac{\delta'_n}{\gamma''_{n-1}}\alpha''_{n-1},\ n \geq 2 \\ \gamma''_n = \gamma'_n - \frac{\delta'_n}{\gamma''_{n-1}}\beta''_{n-1}, \delta''_n = 0,\ n \geq 2. \end{cases} \tag{3.13}$$

For a generic ω this recursion has two linearly independent solutions, which in general will produce divergent sums, and will therefore be incompatible with our boundary conditions. Then, what we we need to do is to find solutions of Eq. 3.12 which satisfy our convergence condition. However, we still need a way of calculating such frequencies (we know how to deal with three-term recurrences, not five), and once we find them we can check the values against our conditions. In order to obtain a useful procedure we first write a recurrence relation for the even and odd coefficients of the series. We start from the odd case, so we want a three-term relation between a_{2n+3}, a_{2n+1} and a_{2n-1}. This can be achieved by writing our three-term recurrence relation for $2n+2$ and $2n$, and eliminating the terms a_{2n} and a_{2n+2}, that is we express a_{2n+2} as a function of a_{2n+1} and a_{2n-1} obtaining

$$a_{2n+2} = -\frac{\beta''_{2n+1}}{\alpha''_{2n+1}} a_{2n+1} + \frac{\gamma''_{2n+1}(\alpha''_{2n} a_{2n+1} + \gamma''_{2n} a_{2n-1})}{\alpha''_{2n+1}\beta''_{2n}}, \tag{3.14}$$

and plugging this result in Eq. 3.12 for $2n+2$. By redefining $d_n = a_{2n+1}$ we obtain

$$\alpha^o_n d_{n+1} + \beta^o_n d_n + \gamma^o_n d_{n-1} = 0,\ n \geq 1, \qquad \begin{cases} \alpha^o_n &= \alpha''_{2n+2}, \\ \beta^o_n &= \gamma''_{2n+2} - \frac{\beta''_{2n+1}\beta''_{2n+2}}{\alpha''_{2n+1}} + \frac{\beta''_{2n+2}\alpha''_{2n}\gamma''_{2n+1}}{\alpha''_{2n+1}\beta''_{2n}}, \\ \gamma^o_n &= \frac{\beta''_{2n+2}\gamma''_{2n}\gamma''_{2n+1}}{\alpha''_{2n+1}\beta''_{2n}}. \end{cases} \tag{3.15}$$

We can also find a similar relation for the even terms ($c_n = a_{2n}$)

$$\alpha^e_n c_{n+1} + \beta^e_n c_n + \gamma^e_n c_{n-1} = 0,\ n \geq 1, \qquad \begin{cases} \alpha^e_n &= \alpha''_{2n+1}, \\ \beta^e_n &= \gamma''_{2n+1} - \frac{\beta''_{2n}\beta''_{2n+1}}{\alpha''_{2n}} + \frac{\beta''_{2n+1}\alpha''_{2n-1}\gamma''_{2n}}{\alpha''_{2n}\beta''_{2n-1}}, \\ \gamma^e_n &= \frac{\beta''_{2n+1}\gamma''_{2n-1}\gamma''_{2n}}{\alpha''_{2n}\beta''_{2n-1}}. \end{cases} \tag{3.16}$$

Now we proceed as we did in the non-extremal case. Our recurrence relations can be associated with continued fractions as in the Leaver case as

$$\frac{a_1}{a_0} = -\frac{\gamma''_1}{\beta''_1 -} \frac{\alpha''_1\gamma''_2}{\beta''_2 -} \frac{\alpha''_2\gamma''_3}{\beta''_3 -} \cdots \tag{3.17}$$

Now, by dividing Eq. 3.6 by a_0 so that we can use our expression for c_1/c_0 and a_1/a_0[1]

$$\alpha_1 \frac{c_1}{c_0} + \beta_1 \frac{a_1}{a_0} + \gamma_1 = -\alpha_1 \frac{\gamma^e_1}{\beta^e_1 -} \frac{\alpha^e_1\gamma^e_2}{\beta^e_2 -} \frac{\alpha^e_2\gamma^e_3}{\beta^e_3 -} \cdots - \beta_1 \frac{\gamma''_1}{\beta''_1 -} \frac{\alpha''_1\gamma''_2}{\beta''_2 -} \frac{\alpha''_2\gamma''_3}{\beta''_3 -} \cdots + \gamma_1 = 0. \tag{3.18}$$

We have not yet mentioned the angular equation 1.42, that is because we have no problems in the extremal limit regarding that equation, meaning we can proceed in the same way as for the non-extremal case, using Leaver's continued fraction, and solving simultaneously equations 3.18 and 2.9. As we said before we cannot study the synchronous frequencies where $M\omega = m/2$, so we limit our study to the investigation of damped modes.

3.2.1.1 Numerical results

We now turn to numerical results. What we find studying the extremal case of damped modes is that the difference between these values and those obtained with Leaver's continued fraction method in the near-extremal case is minimal: [33] shows that for a variety of modes the relative difference between the real part of a mode with $a/M = 0.999$ and an extremal one is $\sim 0.01\%$ (and even less for the imaginary part). This allows us to conclude that not only the transition to extremality seems to be smooth (though we will see this is not always the case), but also that Leaver's method is excellent even for values of the rotational parameter close to the extremal limit. As we have already mentioned, these results do not apply in the case of ZDM. In order to obtain numerical values, we used the same procedure as in the case of non-extremal Kerr, however, we note that finding roots of this new fractions is much more delicate than before.

[1] We believe there is a typo in [33], and in equation 3.11 the apex o should be an e.

As a matter of fact, the absolute value of the function is pretty close to zero in a wide region around QNMs, and we used `Mathematica`'s capability of setting high working precision (higher than machine precision) to find the exact values. As an application of this method we compute the first and second damped modes for ($s = -2$, $l = 2$, $m = 1$). Fig. 3.4 then completes the case we studied before with the strictly extremal values $M\omega = 0.581433 - 0.038255i$ and $M\omega = 0.538855 - 0.118628i$. These results match perfectly the ones found in [33,34] (note that the latter reference uses a different method for calculating these modes).

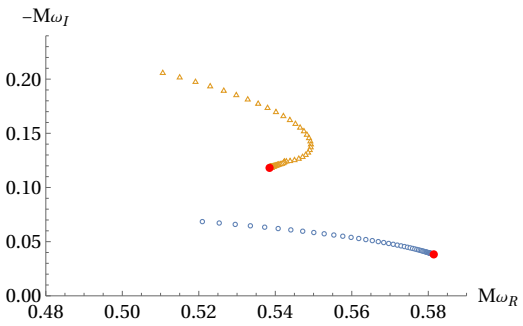

Figure 3.4: In red the extremal values for the first and second damped modes of ($s = -2$, $l = 2$, $m = 1$).

3.2.2 Zero-damping modes and boundary conditions

We have not yet presented a method to calculate ZDM frequencies in the extremal case. Leaver's method does not work when $a/M = 1$, and the modified continued fraction method fails when the frequency equals that of the horizon, that is $\omega = m\Omega_H$, with $\Omega_H = a/2Mr_+$. However, since all ZDMs tend to the same value, we can simply plug that specific value into the Teukolsky equation, which in this case can be solved analytically, and check whether the solutions still satisfy the boundary conditions of our problem. Here we present the argument from [8]. We start by studying how the behaviour of our solution changes at the horizon when we assume the frequency to be $\omega = m\Omega_H$ from the beginning. In this case the horizon is a regular singular point for the wave functions both in the extremal and non-extremal case, meaning we can use Frobenius method to find solutions written as power series around the event horizon. In the non-extremal case, the authors in [8] find the two independent solutions of the radial equation 1.43 to be (we dropped some indices)

$$R_s^I(r) \sim (r - r_+)^{\xi_I}, \quad R_s^{II}(r) \sim Z_s \log(r - r_+) R_s^I(r) + (r - r_+)^{\xi_{II}}, \tag{3.19}$$

where $\xi_I = \max\{0, -s\}$, $\xi_{II} = \min\{0, -s\}$, and $Z_s \neq 0$ is a constant that depends on s. It can also be shown that logarithmic terms are leading only for the case of $s = 0$. For the extremal black hole we have the solutions:

$$R_s^{I,II} \sim (r - M)^{-1/2 - s \pm \delta_s}, \quad \delta_s^2 = \delta_s^2(l, m) = \left(\frac{1}{2} + s\right)^2 - \frac{7}{4}m^2 + A_{lm}\left(\frac{m}{2}\right), \tag{3.20}$$

plus next-to-leading-order corrections, and where the $\pm$ refers to the indices I (+) and II (-) ($A_{lm}(\omega = m/2)$ is the angular separation constant). Since we have defined in Eq. 3.20 δ_s up to a sign, we can assume $\delta_s = \sqrt{\delta_s^2}$, that is, since it is a complex quantity, $\Re(\delta_s) > 0$ in general and $\Im(\delta_s) > 0$ if the real part is zero. We also note that since $A_{lm}^{-s}(m/2) = A_{lm}^{s}(m/2) + 2s$, δ_s is independent of the sign of s. One last propriety of this parameter is that since we are considering a purely real frequency, then $A_{lm}^s(a\omega)$ is also real, and therefore, from its definition, δ_s is either purely real or purely imaginary. Now we have to understand how to formulate our boundary conditions. In general, we can write asymptotic solutions to the radial Teukolsky equation in terms of the tortoise coordinate r_*, defined by $dr_*/dr = (r^2 + a^2)/\Delta$, and the function $Y_s(r) = \Delta^{s/2}\sqrt{r^2 + a^2}R_s(r)$ as:

$$Y_s(r_*) = K_{\text{in}}^{\text{h}}(r - r_+)^{-s/2}e^{-ikr_*} + K_{\text{out}}^{\text{h}}(r - r_+)^{s/2}e^{ikr_*} \tag{3.21}$$

near the event horizon ($r_* \to -\infty$, $r \to r_+$), and

$$Y_s(r_*) = K_{\text{in}}^{\infty} r^s e^{-i\omega r_*} + K_{\text{out}}^{\infty} r^{-s} e^{i\omega r_*} \tag{3.22}$$

far away from the black hole ($r_* \to \infty$, $r \to \infty$), where $k^2 = (\omega - m\Omega_H)^2$ [8]. However, in the case of synchronous frequencies $k = 0$ and we loose the characteristic oscillatory behaviour. Thus, we need a more general kind of boundary conditions, and what we ask is for the wave function to be regular at event horizon, so that the energy-momentum tensor is well behaved and our test field approximation

Synchronous	Extremal	$R_s^I(r)$	$R_s^{II}(r)$	$G_s^I(r)$	$G_s^{II}(r)$
No	No	$(r-r_+)^{-s-iJ_0}$	$(r-r_+)^{iJ_0}$	1	$(r-r_+)^{-s+2iJ_0}$
No	Yes	$e^{\frac{iJ_1}{r-M}}(r-M)^{-2s-2iM\omega}$	$e^{\frac{-iJ_1}{r-M}}(r-M)^{2iM\omega}$	1	$e^{\frac{-2iJ_1}{r-M}}(r-M)^{-2s+4iM\omega}$
Yes	No	$(r-r_+)^{\xi_I}$	$(r-r_+)^{\xi_{II}}$, if $s\neq 0$ $\log(r-r_+)$, if $s=0$	$(r-r_+)^{\xi_I}$	$(r-r_+)^{\xi_{II}}$, if $s\neq 0$ $\log(r-r_+)$, if $s=0$
Yes	Yes	$(r-M)^{-\frac{1}{2}-s+\delta_s}$	$(r-M)^{-\frac{1}{2}-s-\delta_s}$	$(r-M)^{-\frac{1}{2}+im-s+\delta_s}$	$(r-M)^{-\frac{1}{2}+im-s-\delta_s}$

Table 3.1: Table taken from [8]. The different near-horizon behaviors of the field for the two radial functions $R_s(r)$ and $G_s(r)$, defined as $\Upsilon_s = R_s(r)S_s(\theta)e^{im\phi-i\omega t}$ and $\Gamma_s = G_s(r)S_{-s}(\theta)e^{im\tilde{\phi}-i\omega v}$. The parameters are $J_0 = 2Mr_+(\omega - m\Omega_h)/(r_+ - r_-)$, $J_1 = 2M^2(\omega - m\Omega_h)$, $\xi_I = \max\{0,-s\}$, $\xi_{II} = \min\{0,-s\}$, and $\delta_s = \sqrt{\left(\frac{1}{2}+s\right)^2 - \frac{7}{4}m^2 + A_{lm}\left(\frac{m}{2}\right)}$. Logarithmic terms are present in the synchronous, nonextremal cases also when $s\neq 0$, but they are never of leading order near the horizon.

holds. However, we cannot do this using Boyer-Lindquist coordinates (t, r, θ, ϕ), as they are singular at the horizon. One possibility is using ingoing Kerr coordinates $(v, r, \theta, \tilde{\psi})$, defined as

$$dv = dt + \frac{r^2+a^2}{\Delta}dr, \quad d\tilde{\phi} = d\phi + \frac{a}{\Delta}dr. \tag{3.23}$$

We also note that the Kinnersley tetrad which we used to obtain Teukolsky equation is not well behaved at the future event horizon, so we use a tetrad proposed by Hartle and Hawking [35, 36] which we obtain making the substitution $(t \to -t,\ \phi \to -\phi)$. Therefore the function $\Upsilon_s = R_s(r)S_s(\theta)e^{im\phi-i\omega t}$ changes to $\Gamma_s = 2^s\Delta^{-s}\Upsilon_{-s}$. Now we separate these new fields in radial and angular part as $\Gamma_s = G_s(r)S_{-s}(\theta)e^{-i\omega v}e^{im\tilde{\phi}}$, and it can be shown that we can separate the angular equation from the radial one, obtaining the following equation for $G_s(r)$:

$$\Delta\frac{d^2G_s}{dr^2} + [2(s+1)(r-M) - 2iK]\frac{dG_s}{dr} + [-2(2s+1)i\omega r + X_s]G_s = 0, \tag{3.24}$$

where $X_s = 2am\omega - a^2\omega^2 - A_{lm}$ and $K = \omega(r^2+a^2) - am$. We could also use the relation between Υ_s and Γ_s and our change of coordinates to write $G_s(r)$ in terms of $R_s(r)$ as

$$G_s(r) = R_{-s}(r)2^s(r-r_+)^{-s}(r-r_-)^{-s+2iM\omega}\exp\left(i\omega r + 2iMr_+(\omega - m\Omega_H)\int_r\frac{dr'}{\Delta}\right). \tag{3.25}$$

The asymptotic solutions for G_s are analogous with the ones for R_s in the non-extremal case, while for an extremal black hole one gets $G_s^{I,II} \sim (r-M)^{-1/2+im-s\pm\delta_s}$. All these asymptotic behaviours (and some others) are summarized in Table 3.1, taken from [8].

Since the tetrad we have adopted is regular at future event horizon, we can assume as a natural boundary condition that Γ_s (and therefore G_s) must be regular at the event horizon. For a generic solution with $\omega \neq m\Omega_H$ this is the same as imposing an ingoing group velocity at the event horizon, however for synchronous frequencies the former is the only possibility, as the wave character of the solution is lost. Once we have determined the boundary conditions for $G_s(r)$ we can use Eq. 3.25 to determine the boundary conditions on $R_s(r)$. Our most general solution for $G_s(r)$ is of the form

$$G_s(r) = C_s^I G_s^I(r) + C_s^{II} G_s^{II}(r), \tag{3.26}$$

where G_s^I and G_s^{II} are two independent solutions of 3.24 and $C_s^{I,II}$ are constants. We need one last step before formulating our boundary conditions, which has to do with the transformation $s \to -s$. The index s in the Teukolsky equation can be both positive or negative and in both cases the angular and radial equation separate, however, as discussed before, the two equations for $+s$ and $-s$ do not bring different physical information. This means we cannot have Υ_s independent of Υ_{-s} and the same holds for R_s and G_s. The relations between these quantities are the Teukolsky-Starobisnki identities (given in terms of R_s):

$$\mathcal{D}^2R_{-1} = \frac{B_{\rm em}}{2}R_1, \quad (\mathcal{D}^\dagger)^2\Delta R_1 = \frac{2\bar{B}_{\rm em}}{\Delta}R_{-1}, \quad \mathcal{D}^4R_{-2} = \frac{1}{4}B_{\rm grav}R_2, \quad (\mathcal{D}^\dagger)^4\Delta^2R_2 = \frac{4\bar{B}_{\rm grav}}{\Delta^2}R_{-2}. \tag{3.27}$$

where $D = \partial_r - iK/\Delta$, and $D = \partial_r + iK/\Delta$ are differential operators, and $B_{\rm em}$ and $B_{\rm grav}$ are the so called Starobinski-Churilov constants [17]. A consequence of these identities, once applied to our asymptotic formulas for $R_s^{I,II}$ is that $C_s^I \propto C_{-s}^I$ and $C_s^{II} \propto C_s^{II}$ [8]. Now, we can formulate our boundary conditions in terms of C_s^I and $C_s^I I$. Looking at Table 3.1, we see that in all first three cases G_s^I and all its derivatives are always well behaved at the event horizon, while G_s^{II} always diverges for $s \geq 0$, which implies that $C_s^{II} = 0$ for $s \geq 0$. This, together with the relations 3.27, means that $C_s^{II} = 0$ for all values of s. The last case, that is to say synchronous and extremal, must be discussed more in detail. If $m = 0$ then $\omega = 0$, and we can write $A_{lm} = l(l+1) - s(s+1)$ and $\delta_s = l + 1/2$. We have $G_s^I \sim (r-M)^{l-s}$ and $G_s^{II}(r) \sim (r-M)^{-l-s-1}$. Since $l \geq |s|$, then G_s^I is always regular, while G_s^{II} is always irregular. On the other hand, if $m \neq 0$, $G_s^{I,II}$ is regular at the horizon ($r = M$) if and only if $\Re(-1/2 + im - s \pm \delta_s) > 0$, so this means we have two cases:

- $\Re(\delta_s) = 0$ ($\delta_s^2 < 0$), the condition becomes $s < -1/2$, which is automatically satisfied for $s = -1$ and $s = -2$, but never for $s \geq 0$, therefore we need $C_s^I = C_s^{II} = 0$ for $s \geq 0$ which implies $C_s^I = C_s^{II} = 0$ for all s, meaning the only regular solution is the trivial one.
- $\Im(\delta_s) = 0$ ($\delta_s^2 > 0$) our condition becomes $-1/2 - s \pm \delta_s > 0$. For G_s^{II} (the minus sign), we have that the condition cannot be satisfied by positive s, which again implies it can never be satisfied, and thus $C_s^{II} = 0$. Lastly we consider the case of the plus sign, by imposing the regularity of both G_s^I and G_{-s}^I, the conditions that must be satisfied are $\delta_s > 1/2 + s$ and $\delta_s > 1/2 - s$.

Therefore, we can summarize the case $m \neq 0$ with the conditions $\delta_s^2 > 0$ and $\delta_s > 1/2 + |s|$. Since we adopt the convention $\Re(\delta_s) \geq 0$ and we can consider only nonnegative spinweights s, we can write

$$\delta_s^2 > (1/2 + s)^2, \quad s \geq 0. \tag{3.28}$$

If $m = 0$, when the we can write the most general solution to Teukolsky equation as:

$$R_s = A_s(r-M)^{l-s} + B_s(r-M)^{-l-s-1}, \tag{3.29}$$

where A_s and B_s are constants. B_s must be zero to have a well behaved solution at the horizon (just compare this expression with the ones discussed before). However, if $A_s \neq 0$ $R_s(r)$ (and therefore also $G_s(r)$) will diverge at spacial infinity ($r \to \infty$) unless $l = s = 0$. This is clearly true in the case $l \neq s$, and for $l = s > 0$, we can invoke the solution with $-s = -l$ which would diverge at the event horizon. This means that if $M\omega = m = 0$, we can have nonzero solutions which respect our boundary conditions only if these are scalar modes with $l = 0$, whose associated solution is a constant. The argument for $m \neq 0$ is more complicated. The general solution is

$$R_s(r) = (r-M)^{-1-s}\left[A_s \mathcal{M}\left(-im + s, \delta_s; \frac{im(r-M)}{M}\right) + B_s \mathcal{M}\left(-im + s, -\delta_s; \frac{im(r-M)}{M}\right)\right], \tag{3.30}$$

where A_s and B_s are constants and $\mathcal{M}(\beta, \gamma; z)$ is the Whittaker $\mathcal{M}$ function [8]. We can use the asymptotic behaviour of this function $\mathcal{M}(\beta, \gamma; z) \to z^{\gamma+1/2}$ as $z \to 0$ to see how the A_s solution is "related to" R_s^I, while B_s to R_s^{II}. We just derived $B_s = 0$ and $\delta_s > 1/2 + |s|$ for the boundary conditions at the event horizon, now we have to check if it is possible to simultaneously satisfy the conditions for $r \to \infty$. To do so, we use the asymptotic series expansion of the confluent hypergeometric function, giving, far away from the black hole (setting $B_s = 0$),

$$R_s(r) = C_s r^{-1-2s+im} e^{\frac{imr}{2M}} + D_s r^{-1-im} e^{-\frac{-imr}{2M}}, \tag{3.31}$$

where

$$C_s = A_s\left(\frac{im}{M}\right)^{im-s} \frac{e^{-i\frac{m}{2}}\Gamma(1+2\delta_s)}{\Gamma\left(\frac{1}{2} + im - s + \delta_s\right)} \quad D_s = A_s\left(-\frac{im}{M}\right)^{-im+s} \frac{e^{i\frac{m}{2}}(-i)^{-1-2\delta_s}\Gamma(1+2\delta_s)}{\Gamma\left(\frac{1}{2} - im + s + \delta_s\right)}. \tag{3.32}$$

This is a superposition of both ingoing and outgoing waves, whose coefficients are both proportional to A_s, meaning it is impossible to satisfy all our boundary conditions simultaneously. This means that ZDMs are not allowed as natural oscillations in extremal black holes, but they are always associated with scattering modes and should not be classified as (quasi)normal modes [8].

Conclusions

In this thesis we introduced perturbation theory for rotating black holes and calculated the spectra of these systems for different values of the rotational parameter, ranging from the static Schwarzschild case up to the extremal one.

First we introduced the Kerr metric as a solution to Einstein's field equations, and using its symmetries we reduced the problem to one radial and one angular coordinate. Solutions of the angular problem are spin-weighted spheroidal harmonics, and are characterized by two discrete indices l, m. Using Newman-Penrose formalism and Petrov's classification of the Kerr spacetime, we deduced Teukolsky equation, which allows us to describe different kinds of perturbations, scalar, electromagnetic and gravitational, through a single separable partial differential equation. The problem is therefore formulated as two coupled eigenvalue equations, and the eigenvalues of the radial equation give us the quasinormal frequencies. These modes are complex-valued, with negative imaginary part (meaning they are decaying in time), and they are characterized by three discrete indices l, m, n the last one called overtone number, which orders the modes based on their imaginary part.

Afterwards, we presented two methods for computing quasinormal modes for the Kerr spacetime. The first one, Leaver's method, allows us to calculate the frequencies as roots of a continued fraction, and using this technique we computed some spectra of Kerr black holes, away from the extremal limit. The second one is the WKB approximation, which allows us to calculate approximate values of the frequencies in the limit $l \gg 1$ with an analytic expression.

Finally, we presented the near-extremal and extremal cases. As for near-extremal Kerr black holes, we used Leaver's method once again to calculate spectra as $a/M \to 1$. In this regime we recognized two different classes of modes, one in which modes keep a non-zero imaginary part even in the near-extremal limit, called damped modes, and others which, independently of the overtone, all tend to the same purely real value of $M\omega = m/2$, called zero-damping modes. To study the strictly extremal case, we introduced a modified continued fraction method (Leaver's method does not work in this case). This allowed us to extend our previous results for damped modes even in the extremal case, proving that for these frequencies the extremal case is indeed the limit of the near-extremal one and that Leaver's method gives us a very good approximation. As for zero-damping modes, however, this new technique does not work. Since they all tend to the same real frequency, all we had to do was to check whether this value respects our boundary conditions. What we concluded was that this is not the case, and these frequencies are actually associated with scattering modes.

Even though this thesis essentially reproduced existing results in the literature, we did it through independent calculations that combined numerical and analytical methods. It serves as an introduction to black hole quasinormal modes. For a more in-depth study, one could delve into the mathematical aspects of the solutions to Teukolsky equation, or the calculation of the modes in different spacetimes, such as Reissner-Nordström or Kerr-Newman, or different asymptotic metrics, as we only dealt with asymptotically flat spacetimes. Moreover, we only limited our analysis to massless fields, another avenue could be to study a different type of fields (see e.g. [37] for very recent results in this direction). Black holes, particularly in the extremal regime, are valuable testbeds for new theories of gravity, and studying the effect of these theories on quasinormal modes, which are experimentally measurable, could give new insights on the limits of general relativity, making this an active area of research.

Bibliography

[1] D. Cassani, *Advanced lectures on general relativity*, https://userswww.pd.infn.it/ cassani/BlackHoleLectures_2024.pdf.

[2] S. Aretakis, *Dynamics of Extremal Black Holes*, vol. 33 of *SpringerBriefs in Mathematical Physics*, Springer (2018), 10.1007/978-3-319-95183-6.

[3] A. Dabholkar and S. Nampuri, *Quantum black holes*, *Lect. Notes Phys.* **851** (2012) 165 [1208.4814].

[4] E. Berti, V. Cardoso and A.O. Starinets, *Quasinormal modes of black holes and black branes*, *Class. Quant. Grav.* **26** (2009) 163001 [0905.2975].

[5] E. Berti and V. Cardoso, *Webpage with mathematica notebooks and numerical quasinormal mode tables*, *http://www.phy.olemiss.edu/ berti/qnms.html* [http://www.phy.olemiss.edu/ berti/qnms.html].

[6] H. Yang, D.A. Nichols, F. Zhang, A. Zimmerman, Z. Zhang and Y. Chen, *Quasinormal-mode spectrum of Kerr black holes and its geometric interpretation*, *Phys. Rev. D* **86** (2012) 104006 [1207.4253].

[7] H. Yang, A. Zimmerman, A. Zenginoğlu, F. Zhang, E. Berti and Y. Chen, *Quasinormal modes of nearly extremal Kerr spacetimes: spectrum bifurcation and power-law ringdown*, *Phys. Rev. D* **88** (2013) 044047 [1307.8086].

[8] M. Richartz, C.A.R. Herdeiro and E. Berti, *Synchronous frequencies of extremal Kerr black holes: resonances, scattering and stability*, *Phys. Rev. D* **96** (2017) 044034 [1706.01112].

[9] G. Compère and A. Fiorucci, *Advanced Lectures on General Relativity*, 1801.07064.

[10] S.M. Carroll, *Spacetime and Geometry: An Introduction to General Relativity*, Cambridge University Press (7, 2019), 10.1017/9781108770385.

[11] S.A. Teukolsky, *Perturbations of a rotating black hole. 1. Fundamental equations for gravitational electromagnetic and neutrino field perturbations*, *Astrophys. J.* **185** (1973) 635.

[12] E. Newman and R. Penrose, *An Approach to gravitational radiation by a method of spin coefficients*, *J. Math. Phys.* **3** (1962) 566.

[13] A.Z. Petrov, *The classification of spaces defining gravitational fields*, Uchenye Zapiski Kazanskogo Gosudarstvennogo Universiteta im. V. I. Ulyanovicha-Lenina [Scientific Proceedings of Kazan State University, named after V.I. Ulyanov-Lenin], 114, (8) 55-69 (1954)). Jubilee (1804-1954) Collection. (1954) .

[14] O.J.C. Dias, H.S. Reall and J.E. Santos, *Kerr-CFT and gravitational perturbations*, *JHEP* **08** (2009) 101 [0906.2380].

[15] R.P. Geroch, A. Held and R. Penrose, *A space-time calculus based on pairs of null directions*, *J. Math. Phys.* **14** (1973) 874.

[16] R. Gueven, *BLACK HOLES HAVE NO SUPERHAIR*, *Phys. Rev. D* **22** (1980) 2327.

[17] S.A. Teukolsky and W.H. Press, *Perturbations of a rotating black hole. III - Interaction of the hole with gravitational and electromagnet ic radiation*, *Astrophys. J.* **193** (1974) 443.

[18] E. Berti, V. Cardoso and M. Casals, *Eigenvalues and eigenfunctions of spin-weighted spheroidal harmonics in four and higher dimensions*, *Phys. Rev. D* **73** (2006) 024013 [gr-qc/0511111].

[19] E.W. Leaver, *An Analytic representation for the quasi normal modes of Kerr black holes*, *Proc. Roy. Soc. Lond. A* **402** (1985) 285.

[20] G. Arfken, *Mathematical Methods for Physicists*, Academic Press, Inc., San Diego, third ed. (1985).

[21] B.F. Schutz and C.M. Will, *BLACK HOLE NORMAL MODES: A SEMIANALYTIC APPROACH*, *Astrophys. J. Lett.* **291** (1985) L33.

[22] S. Iyer and C.M. Will, *Black Hole Normal Modes: A WKB Approach. 1. Foundations and Application of a Higher Order WKB Analysis of Potential Barrier Scattering*, *Phys. Rev. D* **35** (1987) 3621.

[23] B. Zwiebach, *Mastering Quantum Mechanics: Essentials, Theory, and Applications*, MIT Press (2022), 9780262046138.

[24] C.M. Bender and S.A. Orszag, *Advanced Mathematical Methods for Scientists and Engineers I*, Springer (1999), 10.1007/978-1-4757-3069-2.

[25] R.A. Konoplya, A. Zhidenko and A.F. Zinhailo, *Higher order WKB formula for quasinormal modes and grey-body factors: recipes for quick and accurate calculations*, *Class. Quant. Grav.* **36** (2019) 155002 [1904.10333].

[26] V. Ferrari and B. Mashhoon, *New approach to the quasinormal modes of a black hole*, *Phys. Rev. D* **30** (1984) 295.

[27] G.B. Cook and M. Zalutskiy, *Purely imaginary quasinormal modes of the Kerr geometry*, *Class. Quant. Grav.* **33** (2016) 245008 [1603.09710].

[28] A. Buonanno, G.B. Cook and F. Pretorius, *Inspiral, merger and ring-down of equal-mass black-hole binaries*, *Phys. Rev. D* **75** (2007) 124018 [gr-qc/0610122].

[29] E. Berti, V. Cardoso, J.A. Gonzalez, U. Sperhake, M. Hannam, S. Husa et al., *Inspiral, merger and ringdown of unequal mass black hole binaries: A Multipolar analysis*, *Phys. Rev. D* **76** (2007) 064034 [gr-qc/0703053].

[30] L.C. Stein, *qnm: A Python package for calculating Kerr quasinormal modes, separation constants, and spherical-spheroidal mixing coefficients*, *J. Open Source Softw.* **4** (2019) 1683 [1908.10377].

[31] K.S. Thorne, *Disk accretion onto a black hole. 2. Evolution of the hole.*, *Astrophys. J.* **191** (1974) 507.

[32] Sadowski, A., Bursa, M., Abramowicz, M., Kluźniak, W., Lasota, J.-P., Moderski, R. et al., *Spinning up black holes with super-critical accretion flows*, *AA* **532** (2011) A41.

[33] M. Richartz, *Quasinormal modes of extremal black holes*, *Phys. Rev. D* **93** (2016) 064062 [1509.04260].

[34] M. Casals and L.F. Longo Micchi, *Spectroscopy of extremal and near-extremal Kerr black holes*, *Phys. Rev. D* **99** (2019) 084047 [1901.04586].

[35] S.W. Hawking and J.B. Hartle, *Energy and angular momentum flow into a black hole*, *Commun. Math. Phys.* **27** (1972) 283.

[36] S.A. Teukolsky and W.H. Press, *Perturbations of a rotating black hole. III - Interaction of the hole with gravitational and electromagnet ic radiation*, *Astrophys. J.* **193** (1974) 443.

[37] J.P. Cavalcante, M. Richartz and B.C. da Cunha, *Massive scalar perturbations in Kerr Black Holes: near extremal analysis*, 2408.13964.